Nanocellulose in (bio)sensing

Hamed Golmohammadi[a], Eden Morales-Narváez[b,c], Tina Naghdi[d], Arben Merkoçi[b,e,]*

[a]*Chemistry and Chemical Engineering Research Center of Iran, 14335-186, Tehran, Iran*

[b]*Catalan Institute of Nanoscience and Nanotechnology (ICN2), CSIC and The Barcelona Institute of Science and Technology, Campus UAB, Bellaterra, 08193 Barcelona, Spain*

[c]*Biophotonic Nanosensors Laboratory, Centro de Investigaciones en Óptica, A. C. Loma del Bosque 115, Colonia Lomas del Campestre,37150 León,Guanajuato, México.*

[d]*Young Researchers and Elite Club, Ahvaz Branch, Islamic Azad University, Ahvaz, Iran*

[e]*ICREA, Pg. Lluís Companys 23, 08010 Barcelona, Spain.*

*arben.merkoci@icn2.cat

ABSTRACT

Due to its multifunctional character, nanocellulose (NC) is one of the most interesting nature-based nanomaterials and is attracting attention in a myriad of fields such as biomaterials, engineering, biomedicine, opto/electronic devices, nanocomposites, textiles, cosmetics and food products. Moreover, NC offers a plethora of outstanding properties, including inherent renewability, biodegradability, commercial availability, flexibility, printability, low density, high porosity, optical transparency as well as extraordinary mechanical, thermal and physicochemical properties. Consequently, NC holds unprecedented capabilities which are appealing to the scientific, technologic and industrial community. In this review, we highlight how NC is being tailored and applied in (bio)sensing technology, whose results aim at displaying analytical information related to various fields such as clinical/medical diagnostics, environmental monitoring, food

safety, physical/mechanical sensing, labeling and bioimaging applications. In fact, NC-based platforms could be considered an emerging technology to fabricate efficient, simple, cost-effective and disposable optical/electrical analytical devices for several (bio)sensing applications including health care, diagnostics, environmental monitoring, food quality control, forensic analysis and physical sensing. We foresee that many of the (bio)sensors which are currently based on plastic, glass or conventional paper platforms will be soon transferred to NC and this generation of (bio)sensing platforms could revolutionize the conventional sensing technology.

INTRODUCTION

Nowadays, biosensors represent an outstanding emergent technology that offers advantageous choices -in terms of simplicity, time and cost efficiency- in a wide variety of applications. Biosensing technology aims at revolutionizing the way we measure pivotal parameters related to diagnostics, environmental monitoring, safety and securityand other industrial uses. Consequently, biosensors are taking advantage of novel materials to simplify this technology and improve their overall performance and main characteristics such as sensitivity, specificity and reproducibility.[1–3]

Nanomaterials have extraordinary physicochemical properties that are absent in their bulk counterpart. Hence, over the last decades, nanomaterials have been actively investigated and applied as the core of advantageous (bio)sensing applications.[1–7] Despite several beneficial properties of nanomaterials, their toxicological property on human and environmental health is one of the major concerns for their applications.[8–10]

Recently, the usage of renewable nature-based nanomaterials with biological and environmental benign composition that can be generated using a variety of biomaterials such as synthetic biodegradable polymers, proteins and polysaccharides are being of great interest to tackle these challenges. In this context, among the nature-based nanomaterials, cellulose nanomaterials or nanocelluloses (NCs) have attracted enormous attention during the recent decades as they offer remarkable properties and new opportunities.[11–20] Herein, we discuss how NC is being tailored and applied in (bio)sensing technology along with future outlooks.

Overall Structure, Preparation and Classification of NCs

Cellulose is the most abundant renewable biopolymer available worldwide with an annual production around10^{11}–10^{12} tons. This material can be defined as a linear homopolymer composed of repeating β-D-glucopyranose units that have been linked together by β(1- 4) glycosidic bonds. Cellulose chains with about 36individual cellulose molecules assemble are parallel bound and grouped together through van der Waals forces and hydrogen bonds to form basic structures called elementary fibrils with highly ordered (crystalline) and disordered (amorphous-like) regions, which are aggregated together to form larger units with three-dimensional(3D) networks known as microfibrillated/nanofibrillated cellulose (see Figure 1a).The cellulose fibrils, which have widths in the range of nanometers and lengths of up to several micrometers, are formed during cellulose biosynthesis.[12,13,16–18,21–23]

Typically, cellulose nanofibers (CNFs) can be isolated/purified from cellulose fibers of lignocellulosic resources such as wood and forest/agricultural residues by using various chemical, mechanical or chemo-mechanical processes such as homogenizing, grinding, acid hydrolysis, enzymatic–assisted hydrolysis, (2,2,6,6-Tetramethylpiperidine-1-oxyl)-mediated (or TEMPO-mediated) oxidation, solvent-based isolation, electrospinning and high-intensity ultrasonication.[13,16–18,22,24–26] In other synthetic routes that are especially used for production of bacterial CNFs, they are produced via biosynthesis-generating cellulose and building up bundles of NFs from low-molecular weight carbon sources, such as glucose by cellulose-producing bacteria, such as *Acetobacter G. xylinus* species, now renamed as *Gluconacetobacter xylinus* species.[13,20,24,25,27,28]

In general, depending on the morphological features, functions, and preparation methods of NCs, which in turn rely mainly on the source of cellulosic material and processing conditions, they can be categorized into three main subcategories: cellulose nanocrystals (CNCs), nanofibrillated cellulose (NFCs) and bacterial nanocellulose (BNCs)[16–18,29] (Figures 1b-d, respectively). Various forms of NCs as spherical particles, hydrogels, transparent films/papers and aerogels have also been depicted in Figures 1e-j.

Cellulose nanocrystals (CNCs), also called nanocrystalline celluloses (NCCs), crystallites, (nano)whiskers, rod like cellulose microcrystals, are high purity rod-like or whisker shape cellulose crystals, with nanoscaled diameters and lengths that are usually isolated from cellulose fibers through the removal of amorphous regions by acid hydrolysis or enzymatic-assisted hydrolysis. Due to the lack of amorphous regions in

the structure of CNCs, they are considerably less flexible than other types of NCs.[12,23,30–36]

Nanofibrillated cellulose (NFCs), also known as microfibrillated, nanofibrils, microfibrils, nanofibrillar and nanofibers made of cellulose, are composed of aggregates of long thread-like bundles of cellulose chain molecules with flexible, long and entangled CNFs and endowed with diameters below 100 nm and with lengths of several micrometers. NFCs are usually generated/extracted through the mechanical disintegration processes such as delamination of wood-based cellulose fibers before and/or after enzymatic or chemical treatment. NFCs as electrospun cellulose fibers can also be obtained by using electrospinning technique.[37,38]NFCs have a high aspect ratio and unlike CNCs, contain both crystalline and amorphous regions and exhibit a web-like structure.[13,16,17,25,34,39,40]

Bacterial nanocelluloses (BNCs), also known as bacterial cellulose (BC), microbial cellulose, biocellulose, composed of continuous 3D network of CNFs in the form of randomly assembled ribbon shaped fibrils with diameters less than 100 nm and lengths of several micrometers that are usually produced as hydrogels or nanofilms via “bottom-up” synthetic routes by synthesizing cellulose and building up the fine bundles of NFs from carbon sources such as glucose in the aqueous culture media of specific bacteria such as *Gluconacetobacter xylinus*, as described above, during a time period of days. The BNCs demonstrate better purity, crystallinity and mechanical stability compared to the CNCs and NFCs.[17,28,29,41–43]

The CNFs paper, also called cellulose nanopaper or nanopaper, is usually defined as a sheet completely made of nanosized cellulose fibers. Since the NFs diameter and

spacing are both much less than the visible light wavelength (~one-tenth), the light scattering is considerably suppressed in their nanonetwork; therefore nanopapers exhibit high optical transparency.[44–49]

Properties, Modifications and Applications of NCs

NC offers a plethora of outstanding propertiesincluding inherent renewability, environmental sustainability, biodegradability, simplified end-of-life disposal, unique morphology, excellent chemical-modification capabilities so as to be functionalized, extraordinary mechanical strength (high elastic/Young‘s modulus, high tensile strength and high stiffness), thermal (high thermal stability, very low coefficient of thermal expansion), rheological features (high storage and loss modulus with pseudoplastic and shear-thinning behavior), advantageous optical properties (high optical transparency), high gas permeability and other physicochemical (low density, hydrophilicity, high porosity, high flexibility, high surface area, high crystallinity, etc.) properties.[12,17,18,25,36,46,48,50–54]Due to their multi-performance character and variety of morphologies –e.g., nanocrystals, nanofibrils, nanofilms and electrospun cellulose fibers – and different forms –e.g., papers, transparent films, hydrogels, aerogels, spherical particles, etc–,NCs have acquired increasing attention in numerous applications such as biomaterials engineering, biomedicine, energy (batteries and solar cells), membranes, opto/electronic devices, polymer nanocomposites, textiles and clothing, food, medical, cosmetic and pharmaceutical products, packaging industries, etc.[12,17–19,21,24,25,32–34,42,46,54–68]

In order to improve and also to impart new certain properties to the surface of NCs for desired applications, according to the targeted applications, several strategies have been engineered to tune some interfacial, mechanical and optical properties of NCs and their compatibility, processability and reactivity using wide variety of materials such as hydrophobic matrices and various types of nanoparticles (NPs) and(bio)molecules. The chemical modification or functionalization of the hydroxyl groups onto the surface of NCs can offer specific functional groups via non-covalent surface modification (through adsorption of surfactants, oppositely charged entities/polyelectrolytes), sulfonation, TEMPO-mediated oxidation, esterification, etherification, silylation, urethanization, amidation, click chemistry and polymer grafting.[12–14,22,24,29,32,35,39,53,69–71] In addition, an interesting portfolio of NCs-based composites has been developed. The literature has covered the chemistry, properties, characterization, modifications, production and overall applications of NCs and NCs-based composites.[12–14,16–18,22–26,28,29,32–36,39,40,43,46,53,54,63,69,70,72–75]Herein, we highlight the state-of-the-art on the use of NCs in optical and electrical (bio)sensing and bioimaging, as well as future perspectives and potential applications in the field.

(BIO)SENSING APPLICATIONS OF NCs

The aforementioned outstanding features offered by NCs make them an excellent platform for (bio)sensing applications. In fact, NCs are excellent host substrates and bio-templates/scaffolds for immobilization of guest materials such as various types of plasmonic NPs, photoluminescent NPs, metal NPs, carbon-based nanomaterials,

conductive (nano)materials, biological compounds and fluorescent (bio)molecules for the fabrication of NCs-based organic/inorganic hybrid nanocomposites with extraordinary electrical, optical and mechanical properties[25,28,30,33,42,53,57,62,64,66,75–97] that can be utilized as (bio)sensors for diverse sensing applications displaying analytical information in various fields such as clinical/medical diagnostics, environmental monitoring, food safety, physical sensing and also labeling and bioimaging applications.

NCs-based hybrid materialshave been employed in several (bio)sensing applications so as to detecta variety of different analytes such as gases, biomarkers, drugs, proteins, DNA, pathogens, toxic and hazardous compounds; even in real samples –e.g. environmental, biological or clinical samples—. NCs-based nanocomposites have also been applied in humidity sensing and physical sensing; for instance, strain, proximity and pressure sensors. In the following sections, we will discuss in detail the (bio)sensing applications of NCs.

NCs in Optical (bio)sensing

In this section we highlight the most representative examples related to NCs in optical techniques, including surface enhanced Raman scattering (SERS), colorimetric methods, fluorescent approaches, nanoplasmonic systems and bioluminescence.

SERS has been recently considered as one of the most powerful tools for (bio)chemical detection on account of its high sensitivity and selectivity. Since the molecules are adsorbed at the interstices adjoining metal NPs, so-called “hot spots”, the SERS signal intensity of the adsorbed molecules enhances, because of the strong electromagnetic

field associated with the SPR of metal NPs. The composition, shape, size and interparticle spacing of the noble metallic NPs, intensely affect the strength of the enhancement, owing to their effects on the optical features (e.g. scattering and absorption) of metal NPs. Hence, one of the beneficial ways to maximize the number of hot spots in the SERS sensing applications is the immobilization/synthesis of metal NPs on the porous and flexible substrates. In this regard, NCs, with unique flexible, multilayer and 3D nano-networked scaffold, can be considered as one of the most desirable substrates in SERS sensing. On the other hand, the immobilization of metal NPs on suitable supports is a key step towards the development of (bio)chemical sensors to prevent any undesirable agglomeration/aggregation of metal NPs[98–102].

As far as we are concerned, the first application of NCs in optical sensing was reported by Marques et al. They fabricated silver nanoparticle (AgNP)/BC nanocomposites via *in situ* chemical reduction of adsorbed silver ions onto the BC by citrate method. In this work, BC was applied as a biotemplate for *in situ* growth of AgNPs. The fabricated AgNP/BC nanocomposites were then utilized as an active surface enhanced Raman scattering (SERS) substrate for the determination of thiosalicylic acid and 2,2-dithiodipyridine with a limit of detection (LOD) around10^{-4} M. The performance of AgNP/BC-based SERS substrates for bioanalysis was also assessed in the detection of amino acids such as L-phenylalanine, L-glutamine and L-histidine in aqueous solutions. Additionally, the authors found that in comparison to Ag colloids and other Ag nanocomposites based on vegetable cellulose, AgNP/BC nanocomposites were observed to be more sensitive in SERS applications, which was attributed to the particular microstructure of the BC. In fact, BCs with a 3D ribbon-like nanofibrillar

structure, in comparison to vegetable celluloses with wider cellulosic fibers, provide a greater interfacial area at their surfaces for the deposition of AgNPs, where the adsorbed testing analytes lead to stronger Raman enhancement.[103]

BC hydrogels embedding gold nanoparticles (AuNPs) were fabricated by Park *et al.* through the *in situ* direct chemical reduction of adsorbed gold ions (Au^{3+}) onto the NFs surface of BC to AuNPs by hydroxyl groups of BC fibers. The field emission scanning electron microscopy (FE-SEM) images of fabricated AuNP/BC hydrogels are shown in Figures 2a,b. The fabricated AuNP/BC hydrogels were then used as SERS substrates for the detection of 4-fluorobenzenethiol (4-FBT) and phenyl acetic acid (PAA). The authors also found that the SERS signal intensity could be considerably enhanced (up to 10 times) by spatially deforming/contracting the layered 3D-structure of the AuNP/BC hydrogels in the drying process because of decreasing the distance between AuNPs within BC and subsequently creating SERS hotspots (see Figures2c-e). Interestingly, as schematically shown in Figure 2f the contracting of AuNP/BC hydrogels can also lead to the detection of analytes with low affinity to AuNPs such as PPA, because of the reduced distance between AuNPs and PPA molecules.[100]

Wei *et al*. synthesized AuNP/BC nanocomposites via one step *in situ* chemical reduction of $HAuCl_4$-treated BC by sodium citrate solution. As a high-performance SERS substrate, they applied this hybrid material for the detection of SERS active dyes including, malachite green isothiocyanate (MGITC), Rhodamine 6G (R6G) as well as the herbicide atrazine (ATZ). They found that the $HAuCl_4$ and citrate concentrations affect the AuNPs size and morphology, so that, by increasing the $HAuCl_4$concentration the average size and the total number of synthesized AuNPs within the BC matrix are

increased and their morphology are also changed from uniform Au nanospheres to Au nanoplates. Similar to the work of Park *et al.,*in this study the SERS hot spots were produced as a result of drying the AuNP/BC nanocomposites. Interestingly, an ultra low concentration of MGITC with LOD~24 molecules can be detected by the dried AuNP/BC film. ALOD of 78 nM was also achieved for R6G which indicates that the developed sensor (in dried form) can effectively detect the molecules, even with low affinity to the surface of AuNPs.[101]

Wei *et al*. also used the AuNP/BC nanocomposite as a sensing platform for sensitive and reproducible SERS detection of carbamazepine (CBZ) and ATZ. As shown in Figures 3a,b, the SERS peak intensities are increased by increasing the concentration of analytes. The Raman maps of CBZ, ATZ and blank solutions on AuNP/BC nanocomposite and “SERS barcodes” for MGITC, CBZ and ATZ have also been displayed in Figures3c,d.The developed SERS sensor could detect the analytes quantitatively in the range of 25 nM to 250 µM with LODs of 3 nM and 11 nMfor CBZ and ATZ, respectively. In this study, the affinity of the analytes to the AuNPs embedded in BC was enhanced by lowering the solution pH below the analyte’s pK_a. In a further study, the authors demonstrated the broad applicability of the fabricated sensing platform for the detection of five additional analytes with low pK_a (melamine, 2,4-dichloroaniline, 4-chloroaniline, 3-bromoaniline and 3-nitroaniline).[102] Although several research teams have exploited NCs as a SERS substrate, the modification of NCs with nanoparticles maximizing the SERS effect (such as nanostars or nanorods) has been scarcely explored. Additionally, both detection of complex molecules such as proteins

and detection of analytes in real matrices have also been scarcely studied using SERS substrates based on NCs.

CNCs labeled with pH responsive fluorescent dyes (isothiocyanate and succinimidyl ester dyes) could be successfully utilized for pH sensing. A simple one-pot procedure in basic media was used for fluorescent labeling of CNCs with isothiocyanate dyes (see Figure 4a). Alternatively, the succinimidyl ester dyes were covalently grafted onto the surface of CNCs, which were amine-functionalized via esterification reaction followed by a thiol–ene Michael addition. The pH responsiveness of the fluorescently labeled CNCs was verified by suspending them in buffer solutions ranging from pH 3.5 to pH 8.0, for the isothiocyanate dyes labeled CNCs (see Figure 4b),from pH4.0 to 8.5 and from pH 2.6 to 7.0 for two different succinimidyl ester dyes-labeled CNCs.[104]

Davarayn and Kim developed an eco-friendly pH sensor by immobilizing a natural pigment (from red cabbage) onto the electrospun CNFs through adsorption and then chemical cross-linking reaction using a bifunctional cross-linker reagent (hexamethylenediisocyanate). The biocomposite-based pH sensor is reversible, recyclable, stable (under different temperatures at three different pHs 2, 5, and 10, and at prolonged storage time for over 1 month at room temperature) and also universal as it displays different colors for each pH value in the range of 1-14 (see Figures4c,d). Owing to these advantages, the authors suggest that it can be exploited as a diagnosis tool for health monitoring (e.g. to evaluate the certain illnesses such as infectious and digestive diseases and some types of cancer, or even diagnosis of alcoholic persons,

etc) because the pH changes of human biological fluids such as blood, urine, salvia, etc. can represent the status of many biological systems and processes.[105]

The grafting of fluorescent poly(amidoamine) (PAMAM) dendrimers onto the surface of CNCs through carbodiimide-mediated amidation process and the pH-responsive and fluorescent behaviors of the resulting PAMAM/CNC have been reported by Chen *et al*. The fluorescent behavior of the synthesized composite material was mainly affected by the formation of aggregates. Stable dispersions of PAMAM-CNC with strong blue fluorescent emission were obtained at highly acidic ($pH \leq 4$) or basic ($pH \geq 10$) aqueous media where the large aggregates were not formed due to electrostatic attractions (see Figure 4e). Owing to the pH-responsive and fluorescent properties of the proposed material, the authors suggested that it could be potentially applied in pH responsive nanodevices, optical markers, fluorescence based sensors and nanoreactors.[106] Likewise, Tang *et al*. proposed CNCs covalently conjugated with a pH-indicator dye (5 (and 6)-carboxy-2',7'-dichlorofluorescein) via an amidation reaction, with an amino acid spacer linking (L-leucine). The attachment of spacer linker onto the surface of CNCs can effectively avoid the self-aggregation of CNCs. The fluorescence intensity of fabricated pH-sensitive CNCs was increased upon increasing of pH value from 2.28 to 10.84.[107]

Interestingly, light-emitting non-water-soluble compounds such as poly(9,9-dioctylfluorene) (PFO) can be encapsulated by self-assembled nanomicells made of amphiphilic cellulose, leading to a water-soluble fluorescent nanocellulose-based hybrid. The fabricated fluorescent PFO/amphiphilic cellulose nanoa ggregates can be then utilized for detection of nitroaromatic explosives (NACs) such as 2,4,6-

trinitrophenol (picric acid or PA), 2,4-dinitrotoluene (DNT) and 2,4,6-trinitrotoluene (TNT) in aqueous solutions via fluorescence quenching mechanism between the proposed composite as energy donor and NACs as energy acceptors. Wang et al. demonstrated that the sensitivity of the designed water-soluble composite towards NACs has been dramatically enhanced (over 50-fold) in comparison with PFO in organic solvent, which was attributed to the maximized interaction between PFO and NACs within the cellulose-based nanoaggregates.[108]

Edwards *et al*. have reported a colorimetric and fluorimetric method for human neutrophil elastase (HNE) sensing by using peptide-linked cotton CNCs.– During inflammation, HNE is secreted by neutrophils and macrophages so as to destroy bacteria and host tissue. For the design and preparation of this sensor targeting HNE, n-Succinyl-Alanine–Alanine-Valine-paranitroanilide (Suc-Ala–Ala-Val-pNA) was covalently immobilized on glycine esterified CNC as a HNE tripeptide. The enzymatic release of chromogen para-nitroaniline from the peptide-conjugated CNC in the presence of HNE and subsequently its reaction with color amplifying reagents enhancing the visible absorption of the chromogen was employed as sensing strategy for colorimetric/fluorimetric detection of HNE. In the developed method, the immobilization of peptide substrate on the CNC surface has increased the surface area, sensor sensitivity and accessible peptide substrate efficacy.[109]

Edwards *et al.* also reported the synthesis, characterization of fluorescent analogs and structure/function analysis of peptide biosensors conjugated to cellulosic and nanocellulosic materials that applied for fluorescence detection of HNE as low as 0.05 U/mL in chronic wounds. The authors again found that among the cellulosic and

nanocellulosic based HNE biosensors, the CNC based biosensors, presented the highest sensitivity towards HNE due to their high surface area.[110]

Functional scaffolds based on CNCs and polyvinyl alcohol (PVA) have been developed by Schyrr *et al.* and proposed as fluorescence-based sensing platforms. Thin films of porous the PVA/CNC nanocomposite were deposited by dip-coating on glass substrates and then attached by heat-treatment. The deposited films were then functionalized with 2-(acryloxy)ethyl (3-isocyanato-4-methylphenyl)carbamate to produce the acrylated porous PVA/CNC nanocomposite films that can be afterwards used via thiol-ene reactions to immobilize any thiolated sensing motif.The resulting scaffold was first exploited for pH-sensing after immobilizing a fluorescein derivative (thiolated fluorescein-substituted lysine)on the surface of acrylated scaffold. The fluorescence response of the designed pH sensor was extremely rapid. The performance of the resulting scaffold was also applied for protease activity detection by immobilizing a thiolated fluorogenic peptide (FP-SH) via a peptide sequence on the acrylated scaffold. The sensing strategy of this sensor (FP-SH/PVP/CNC) is based on the cleavage of the peptide sequence that in the presence of protease enzyme will trigger the release of the quencher from the surface of the sensor and subsequently recovering the quenched fluorescence.[111]

Zhou et al. have developed a multifunctional glyconanomaterial platform based on CNCs for lectin recognition. In this study, the carboxylated CNCs (CCNCs) were dually functionalized with a fluorescent dye(quinolone) and two carbohydrate ligands(Figure 5a). The fluorescence intensity of the multifunctional fluorescent CCNCs was significantly decreased in the presence of lectin. Furthermore, the authors demonstrated

that the multifunctional fluorescent CCNCs could be utilized as bacterial affinity probes for Escherichia coli (*E. coli*) imaging by targeting lectin receptors at the surface of the bacterial cells (Figures5b,c). The noteworthy advantage of the developed method is the use of the CCNCs as nanomaterials with low cytotoxicities toward human cells and tissues compared to other reported nanomaterials with high potential cytotoxicities that have previously been applied as glyconanomaterial platforms.[112]

Recently, the authors of this review article have developed various nanopaper-based nanocomposites by embedding different plasmonic and photoluminescent NPs within the scaffold of BC nanopaper. The plasmonic and photoluminescence nanopaper-based nanocomposites were fabricated using three routes, which are depicted in Figures 6a-d. We exploit the hydroxyl reactive groups of the BC as a reducing agent for *in-situ* chemical synthesis of AgNPs within transparent BC nanopaper (Route a; see Figure 6a). The authors also utilize BCs as a biotemplate/scaffold to embed AuNPs using a reducing agent during their synthesis (Route b; see Figure 6b). Alternatively, the authors attach protein/amino-functionalized photoluminescent NPs such as streptavidin-coated CdSe@ZnS quantum dots (QDs), aminosilica-coated NaYF4:Yb^{3+}@Er^{3+} up-conversion NPs (UCNPs) and other aminated photoluminescent (nano)materials such as amine-functionalized carbon dots, photoluminescent graphene oxide, trypan blue and rhodamine onto BCs that were previously carboxylated using a TEMPO-mediated oxidation system (Route c; Figures6c,d).It was also demonstrated that BC nanopaper can be easily patterned according to different shapes or hydrophobic barriers, by using a wax printing machine or punch tools, to generate useful devices, including 2D cuvettes, 2D microwell plates, and spots for individual assays (Figure 6e).The authors

also reported that the photoluminescent or plasmonic properties of the fabricated nanopaper-based nanocomposites can be significantly modulated using different analytes to perform analytical tasks, including as 2-mercaptobenzothiazole (MBT), cyanide, iodide, thiourea, methimazol, *E.coli* and ammonia detection. As representative instances of some possible applications of the fabricated plasmonic nanopapers, the AgNP/BCwas exploited as a chemoprobe for optical monitoring of 2-mercaptobenzothiazole (MBT) and cyanide ion in water samples. The fabrication process of plasmonic nanopaper and its application for colorimetric monitoring of MBT and cyanideare depicted in Figure 7a**.**As shown in Figure 7b, by increasing the concentration of cyanide, the intensity of the localized surface plasmon resonance (LSPR) absorption band of AgNP/BC nanopaper has been significantly decreased with a blue-shift to shorter wavelengths and consequently their color has been obviously changed from amber to light yellow, due to an etching process in the embedded AgNPs, which is shown in Figures 7g-3.Aside from this, upon the addition of MBT concentration, the color of AgNP/BC has been changed to dark brown color and subsequently the intensity of their LSPR absorption band has been dramatically decreased with a red shift to longer wavelengths (see Figure 7c), owing to the aggregation of AgNPs embedded within BC nanopaper (see Figure 7g-2).The sensing strategy for the colorimetric sensing of MBT and cyanide is based on the strong affinity of the thiol groups of MBT and cyanide towards the surface of the AgNPs embedded within BC nanopaper that would eventually lead to changes in their LSPR properties and the color of the reported plasmonic nanopaper. This plasmonic nanosensor can detect the analytes quantitatively, in the range of 2-110 µg mL^{-1} and 0.2-2.5 µg mL^{-1} with a LOD

1.37 µg mL^{-1} and 0.012µg $mL^{-1}$for MBT and cyanide, respectively.[85] The fabricated AgNP/BC was further utilized as a colorimetric-based sensing platform for the detection of methimazole and iodide, in the range of 0.5-10 µg mL^{-1} and 0.2-4 µg mL^{-1},respectively.[77] We also exploited AuNP/BC as a colorimetric sensor for the detection of thiourea and cyanide in water samples, in the range of 2-8 µg mL^{-1} and 0.5-4.5 µg mL^{-1}, respectively (see Figures7c,d, respectively). The scanning electron micrographs of AuNP/BC, in the presence of thiourea and cyanide are shown in Figure 7h.

The photoluminescence of QD/BC and UCNP/BC embedded in BC can also be modulated using graphene oxide (GO) as a universal long-range photoluminescence quencher. As can be seen in Figures8b-e, the photoluminescence intensity of QD/BC and UCNP/BC has been significantly quenched upon the addition of GO. In addition, the authors decorate QD/BC with antibodies targeting a large-sized analyte, that is, *E. coli* so as to use GO as a pathogen-revealing agent via fluorescence resonance energy transfer (FRET).Since FRET strongly depends on the distance between the involved photoexcited donors (antibody-decorated QD/BC) and the involved FRET acceptor (GO), upon addition of GO, the donors will display a strong photoluminescence emission in the presence of the large-sized analyte, whereas the donors will be quenched in the absence of the large-sized analyte (see Figures8f-h).Moreover, the authors demonstrate that BC nanopaper, in comparison with other conventional paper substrates (e.g.nitro/cellulose), could be utilized as an advantageous preconcentration platform/membrane that facilitates the analysis of small volumes (~4 µL) of optically active materials. The scanning electron micrographs of the reported nanopaper-based platforms are shown in Figures8i-l.[77]

Apart from this, it was also demonstrated that AgNP/BC bionanocomposite is amenable to detecting analytes in the gas phase. Interestingly, this hybrid material can be utilized as a nanoplasmonic sensor for visual detection of ammonia. The authors found that AgNPs embedded within BC are partially or entirely etched when exposed to ammonia vapor. Hence, the population density of the AgNPs decreases and the interparticle distance increases, leading to a decrease in the intensity of LSPR absorption spectra of the embedded AgNPs and a change in color from amber to light amber, which can even be visually determined. We also discovered that the size distribution of AgNPs embedded in BC is dramatically modulated showing a change in color from amber to grey or taupe in the presence of volatile compounds released during meat and fish spoilage, respectively (see Figure 9). The designed nanoplasmonic sensor has a great potential for smart packaging and other gas sensing-related applications.[113]

Ruiz-Palomero et al. have applied β-cyclodextrin-decorated NC as a supermolecular sorbent in a solid phase microextraction (SPME) method for the selective fluorimetric determination of danofloxacin (DAN, a fluoroquinolone antibiotic). A β-cyclodextrin was covalently attached to amine-functionalized NC via amidation reaction. The developed SPME platform exhibited satisfactory reproducibility, reusability, selectivity and linearity within a concentration range from 8 to 800 μg L^{-1}, and a LOD of 2.5 μg L^{-1}. This system was also successfully employed in the fluorimetric recognition of DAN in milk samples with satisfactory recoveries.[114]

The same research team has also fabricated highly photoluminescence gels by embedding Ru(II) bipyridine complex as a luminophore and sensitizer in the carboxylated NC hydrogels, leading to an efficient analytical tool for AgNPs sensing. As

a sensing mechanism, the photoluminscent gel matrix can be quenched upon addition of AgNPs owing to the electrostatic interaction between the ion pair electrons of the amine group of Ru(II) and the cationic groups of AgNPs. The incorporation of Ru(II)-complex moieties in the 3D scaffold of NC hydrogel considerably enhanced the sensing signal (in comparison with Ru(II)-complex in aqueous solution) and specificity towards AgNPs owing to the electrostatic interaction of the anionic groups of carboxilated NC and the cationic amine groups of the Ru(II) complex. This sensing platform demonstrated a good reproducibility, selectivity and linearity in the concentration range from 18.5 μM to 148 μM with a LOD of 11.1 μM. This system was successfully utilized for the analysis of AgNPs in two real samples, deodorant and socks labelled with AgNPs, with acceptable recovery within the range of 83.7-94.2%.[115]

Aiming at determining toxicity in liquid samples, BC nanopaper can also be decorated with bioluminescent bacteria (*Aliivibrio fischeri*), whose luminescence can be inhibited in the presence of toxic compounds such as herbicides, pesticides and flame retardants, as reported by Liu et al.[116] Since BC promotes bacterial proliferation, the aforementioned bioluminescent bacteria can be easily cultured *in situ*, leading to a simple and cost-effective paper-based device for rapid screening of hazardous compounds even in real matrices such as lake and marine water.

NCs in Bioimaging

Owing to their lack of cytotoxicity, biocompatibility, biodegradability and excellent functionalization abilities, fluorescently labeled NCs have been applied for the generation of emergent medical diagnostic tools– mainly used as carriers.

A potential bioimaging and bioassay application of NCs was firstly reported by Dong and Roman. They covalently attachedfluorescein-5-isothiocyanate (FITC) to the surface of CNCs via a three-step reaction pathway, involving creation of primary amino groups on the CNCs surface and then coupling of FITC molecules to the aminated CNCs. The authors suggested that fluorescently labeled CNCs could be potentially exploited to study the interaction of CNCs with cells and the biodistribution of CNCs *in vivo*, which is very important for biomedical applications of NCs.[117]Theyalso synthesized folic acid-conjugated CNCs and applied them for cancer targeting. The folic acid was conjugated to FITC labeled CNCs (see Figure 10a) and then utilized for selective targeting of the folate receptor-positive human and rat brain tumor cells (see Figure 10b).[118]Additionally, Grate *et al,* have covalently incorporated Alexa Fluor dyes onto the surface of CNCs using two different approaches for bioimaging applications. The Alexa Fluor-labeled fluorescent CNCs were deposited in polydimethylsiloxane, as a pore network microfluidic structure, and then the spatially localized solid cellulose materials was applied in microenvironments for bioimaging. They were also applied to observe and follow their disappearance under the action of hydrolytic enzymes or living microorganisms (see Figures10c,d).[119] In addition, Colombo *et al.*, evaluated the interaction of CNCs with living organisms and followed them in living animals (healthy mice). The CNCs were covalently labeled with a fluorescent dye, Alexa Fluor 633, which can be detected by *in vivo* optical imaging (see Figure 10e)[120].Navarro *et al,* fabricated

a luminescent NC platform by labeling a graft blockcopolymer-modified CNF with a Lucifer yellow derivative and exploited this material for fluorescence-based optical sensing. The CNF uptake and biodistribution in living organisms such as *Daphnia magna* was followed via optical imaging(see Figure 10f).[121]

It is worth mentioning that although this branch of research focused on the generation of NCs-based materials facilitating bioimaging is progressing, as far as we are concerned, theranostic approaches based on NCs allowing for therapy and diagnostics in tandem have been little explored until now.

NCs in Electrical (bio)sensing

NC-based platforms are expected to be conductive in electrical sensing devices so as they can give an electrical response. Considering that NCs are inherently non-conductive, various types of modifying agents have been used to make them conductive; for instance, introducing conducting electroactive (nano)materials into their matrix[75,97]. In fact, there have been substantial efforts to develop NC-based electrical sensing devices. Bonne *et al*. demonstrated for the first time the application of cellulose nanomaterials for electrical sensing targets. They modified the surface of glassy carbon electrodes (GCE) with thin films of reconstituted CNFs, which were modified with embedded receptors. A solvent evaporation technique was utilized to form thin CNFs films. An aqueous solution of CNFs was deposited onto a GCE, and kept at 60 °C for 20 min. Evaporation of an aqueous solution of CNFs onto GCE surfaces resulted in a stable and uniform film coating. In the modified electrode, CNFs were employed as inert

backbone and poly-(diallyldimethylammonium chloride) or PDDAC as a polycationic receptor to introduce selective binding sites for the transport and accumulation of anions and particularly hydrophobic anions. The electrochemical properties of the PDDAC/CNFs film electrodes were first investigated for a model redox system ($Fe(CN)_6^{3-/4-}$) and then for the determination of triclosan –a hydrophobic polychlorinated phenol which is widely used as a biocide. The authors showed that triclosan can be detected in the concentration range of 10^{-6}-10^{-3}M by their proposed method.[122] The same research team modified the surface of GCE with a thin film of CNFs/chitosan composite (chitosan was utilized as a molecular binding site or "receptor"). Owing to the relatively high affinity of sodium dodecylsulfate (SDS) to the CNFs/chitosan composite, the authors suggested that the CNFs/chitosan modified electrode could be potentially used for the accumulation and electrochemical detection of SDS and other anionic surfactants.[123]

Hydrogen peroxide and glucose have also been detected using hybrid materials such as AuNPs/NCs.[96,124,125] The fabrication of AuNP/BC nanocomposites through a one-step biotemplated method by using poly(ethyleneimine) (PEI) as a linking and reducing agent for the synthesis of AuNPs within the scaffold of BC was first described by Zhang et al. The fabricated AuNP/BC nanocomposites were found to be excellent supports for enzyme immobilization. Therefore, the as-prepared AuNP/BC nanocomposites, which have been coated on the surface of GCE, were functionalized with horseradish peroxidase (HRP) as a model enzyme so as to produce a H_2O_2 biosensor. The GCE was first polished using alumina slurry and then rinsed thoroughly with water and ethanol followed by drying by nitrogen. A dispersion of synthesized AuNP/BC was

dropped on the pretreated GCE and then dried at room temperature. The AuNP/BC modified GCE was then incubated with HRP solution in a humidity chamber at 4 °C overnight. The resultant HRP/AuNP/BC/GCE exhibited excellent bioactivity in the reduction of H_2O_2 and was applied for amperometric detection of $H_2O_2$with a LOD lower than 1 µM.[96]

Moreover, Wang et al. constructed a glucose biosensor based on the immobilization of two enzymes, glucose oxidase (GOx) and HRP on the surface of the fabricated AuNP/BC/GCE while remaining their bioactivity activities. The pretreated GCE was modified by coating of the AuNP/BC suspension which was dispersed in isopropanol and then dried in air at room temperature. The modified electrode (AuNP/BC/GCE) was cast with a phosphate buffer solution containing HRP, GOx and PDDA at 4 °C for 12 hours. The constructed bienzymatic glucose biosensor exhibited satisfactory stability, reproducibility, selectivity and linearity in the concentration range from 10 µM to 400 µM with a LOD of 2.3 µM and was successfully applied in the determination of glucose in human blood samples with satisfactory results.[124]

Wang *et al*. also developed amperometric H_2O_2biosensorsbyembeddingheme proteins such as HRP, hemoglobin (HB) and myoglobin (MB) into the nanonetwork scaffold of the fabricated AuNP/BC/GCE.The electrocatalytic activities of the fabricated heme protein/AuNP/BC/GCE for the reduction of H_2O_2 were evaluated in the presence of hydroquinone (HQ) as an electron mediator. The authors found that among the fabricated H_2O_2biosensors, the HRP/AuNP/BC/GCE presented the highest biocatalytic activity and a rapid amperometric response toward H_2O_2,with a wide dynamic range from 0.3 µM to 1.0 mM and a low LOD around 0.1 µM.[125] Likewise, Dong *et al.*

deposited AuNPs on positively charged functional groups of poly(diallyldimethylammonium chloride)/CNC (PDDAC/CNC) via *in situ* chemical reduction of adsorbed negative Au precursors($AuCl_4^-$) by $NaBH_4$.Thesurface of GCEs was then modified with the explored AuNP/PDDA/CNC nanohybrids. The modified electrodes were then utilized as an electrochemical biosensor for non-enzymatic glucose sensing and exhibited a high linear amperometric response ranging from 0.004 mM to 6.5mM with a high sensitivity (*ca.* 62.8μA·mM^{-1})and a LOD of 2.4μM glucose.[126]

The fabrication of a glucose biosensor via covalent immobilization of GOx enzyme onto a polypyrrole/cellulose nanocrystal (PPy/CNC) membrane has been described by Esmaeili *et al*. The electrochemical analysis showed that the nature and biocatalytic activity of GOx enzyme immobilized on the PPy/CNC were retained. This biosensor targeting glucose exhibited fast electron transfer, good stability, reproducibility and linearity within the concentration range from 1.0 to 20 mM with high sensitivity (*ca*. 0.73 μA·mM^{-1}) and a LOD of 0.05 mM.[127]

Liu et al. fabricated AgNP-carboxylated cellulose nanocrystals based nanocomposites (AgNP/CCNC)by the chemical reduction of adsorbed Ag^+ onto CCNCs using $NaBH_4$. A DNA probe was grafted on the fabricated AgNP/CCNC by the amide linkage. The resultant nanocomposites (decorated with DNA) were employed for sensitive and selective detection of the complementary target DNA sequence. The electroreduction of Ag^+ ions was used as an analytical response for the electrical identification of DNA hybridization. Ag^+ ions are released from the AgNPs anchored onto the hybrids as a result of the occurred hybridization (between the target DNA and the probe grafted on the fabricated AgNP/CCNC, which leads to a modulation of the differential pulse anodic

stripping voltammetry (DPASV) of the developed biosensor. A linear calibration curve was observed for phosphinothricin acetyltransferase (PAT) gene sequence over a concentration range of 1.0×10^{-10} to 1.0×10^{-7} M with a LOD of 2.3×10^{-11}M.[128] Likewise, this strategy was used to fabricate Ag–Pd NPs alloy/CCNC nanocomposites and were then applied for the electrochemical detection of phosphoenolpyruvate (PEP) gene sequence.[129]

Hu and colleagues have developed a formaldehyde sensor based on PEI/BC membranes-coated quartz crystal microbalance (QCM). In general, QCM sensor can be fabricated via coating the surface of a quartz crystal electrode with a membrane which is able to interact with the target materials in the environment. To fabricate the QCM sensor for determination of formaldehyde, a quartz crystal was first rinsed with deionized water and ethanol and subsequently dried at room temperature. A treated mixture of BC suspension was then dispensed onto the surface of the quartz crystal electrode and dried. PEI/BC membranes coated QCM were then constructed via dripping a PEI solution on the BC coated QCM and eventually dried. In the fabricated QCM sensor, BC was employed as a 3D nanofibrous membrane with high porosity and surface area that can enhance the sensor sensitivity due to an increase in the specific surface area of PEI which acts as sensing material. The reversible interaction between the amine groups of PEI and the formaldehyde molecules, which leads to decrease the frequency of the fabricated QCM sensor upon the addition of formaldehyde concentration, was recommended as sensing strategy for determination of formaldehyde. The developed QCM sensor exhibited a high reversibility and reproducibility with a linear response that is sensitive to mass changes of formaldehyde

vapors in the range of 1-100 µg mL^{-1} with a LOD of 1 µg mL^{-1}.[130]The same research team reported a humidity sensor based on BC-coated QCM. In this approach, BC was used as sensitive coating for humidity detection. They demonstrated that the humidity sensitivity of the fabricated QCM sensor has been considerably enhanced (up to 4 times) at 97% relative humidity (RH) compared with cellulose membranes due to a larger specific surface area offered by the ultrafine 3Dnanonetwork scaffold of BC. The developed QCM sensor showed good long-term stability and reversibility and exhibited a good linearity towards RH ranging from 20% to 97%.[131]

Strain sensors are utilized to transduce/transform mechanical deformations into electrical signals (changes of resistance or capacitance) and have found a wide variety of applications for their promising potentials in interactive electronics, robotic systems, implantable medical devices, human motion detection, human-machine interfaces beside others.[132–134]

Farjana *et al*. investigated the strain sensitivity of flexible and electrically conductive nanocomposites that have been fabricated by the treatment of BCs with double-walled carbon nanotubes (DWCNTs) and multi-walled carbon nanotubes (MWCNTs). The conductivity of the fabricated strain sensors ranged from 0.034 $S.cm^{-1}$ to 0.39 $S.cm^{-1}$ and from 0.12 $S.cm^{-1}$ to 1.6 $S.cm^{-1}$for DWCNT/BC and MWCNT/BC, respectively. In order to evaluate the strain sensitivity of the fabricated conductive BCs, their strain-oriented electromechanical features and responses (electrical resistance versus strain) were measured during the application of tensile force. The authors found that the strain sensitivity of the fabricated conductive BCs depends on their conductivity and increases

upon increasing the conductivity of samples, so that MWCNT/BC with high conductivity shows higher strain sensitivity than DWCNT/BC.[97]

Wang *et al*, fabricated hybrid nanocomposite aerogels by combining the extraordinary mechanical properties, easy processing and the abundant availability of NFCs and the attractive electrical features of CNTs aerogels in a synergistic way. To fabricate the CNT/NFC hydrogel, an aqueous dispersion of functionalized CNT was first added into the prepared NFC hydrogel and then mixed with a high speed mixer and ultrasonic bath. The hybrid conductive CNT/NFC aerogels were eventually freeze-dried from aqueous hybrid gels. The morphology of fabricated aerogels can be tuned through controlling the freeze-drying process. Owing to the sponge-like structure of fabricated conductive CNT/NFC aerogels, their electrical properties (resistance or conductivity) can be changed upon imposing the pressure. Hence, the elastic mechanical properties and electrically reversible compressional behavior of the fabricated hybrid conductive nanocomposites were applied for mechano-responsive conductivity and pressure sensing.[135]

Mesoporus nanopaper has also been reported to be an advantageous platform for (bio)sensing applications, this material is composed of a thin layer of nanopaper film with an extraordinary surface roughness and a thick layer of hardwood fibrous network with excellent liquid absorption ability. Bao *et al*, utilized a bilayer mesoporous nanopaper to develop a high-performance liquid electrolyte-based transistor via deposition of 2D van der Waals materials (MoS_2, graphene). The source, drain, and gate contacts were deposited onto the smooth side of the nanopaper, whereas the mesoporous side of the bilayer nanopaper was used as a reservoir to quickly absorb

electrolyte(Figures 11a-d). The liquid-based application of the designed graphene-based transistor was then applied for electrical pH sensing. As shown in Figures 11e-f,the Dirac point of the designed transistor was shifted to the positive direction upon pH value increasing from 1.7 to 9.3, which is attributed to the attachment of hydroxide ions acting as electron scavengers and making graphene more p-doped. The authors suggested that their fabricated liquid-gated transistors could also be potentially exploited for diverse (bio)sensing applications[89].

Other electrochemical approaches have been developed by Shahrokhian *et al*., who propose, the immobilization of the composite cellulose nanofibers/carbon nanoparticles (CNFs/CNPs) on a glassy carbon electrode (CNFs/CNPs/GCE) for voltammetric determination of clonazepam (CLNP) and metoclopramide (MCP).The results of this voltammetric analysis demonstrated that due to the increase of the electroactive surface area, the peak current of CLNP and MCP onto the surface of CNFs/CNPs/GCE have been remarkably enhanced (up to 60 times and 49 times for CLNP and MCP, respectively) compared to the bare GCE. The developed electrochemical sensors showed high sensitivity, stability, reproducibility, repeatability and linearity in a wide concentration range, from 0.1-10 µM and 0.06-2 µM with a low LOD of 80 nM and 6 nM for CLNP and MCP, respectively. In addition, this approach was successfully employed for quantitative analysis of CLNP and MCP in pharmaceutical and clinical preparations.[136,137]

Sadasivuni *et al.* have developed a flexible and transparent CNC/modified-reduced graphene oxide (CNC/m-rGO) film for proximity sensing (sensitivity without any physical contact). The CNC/m-rGO films were fabricated via layer-by-layer spraying of m-rGO

filled CNCs on interdigitated electrodes (containing lithographic patterns on epoxy film substrates). The fabricated CNC/GO-based proximity sensor can detect a human finger interface with a short-distance sensing capability (around 6 mm) and a suitable recovery time interval. This proximity sensor can be explored in electronics, optoelectronics, robotics, mobile phones, punching machines and other applications.[138]

Yan *et al*, fabricated a high strain sensor based on a nanocomposite of crumpled graphene and nanopaper that were embedded in polydimethylsiloxan (PDMS) as a stretchable elastomer matrix. The images of the free-standing state of the stretchable strain sensor, and their capability for all-directional (X, Y and Z directions)strain sensing and corresponding response behaviors are shown in Figures 12a-h.Interestingly, the fabricated highly stretchable piezoresistive sensor based on graphene and nanopaper is capable for the detection of high strain with a detection limit up to 100%.In the fabricated strain sensor, NC as a green, low-cost and efficient “binder” increases the processability of crumpled graphene. The fabricated sensor was also applied as a wearable strain sensor for human-motion detection (to detect the stretching and bending of fingers) (see Figures12i,j).[139]

Zhong *et al*, designed a transparent nanopaper based-self powered and human interactive flexible system which is composed of two transparent components, CNTs/transparent nanopaper (T-paper) and polyethylene (PE)/CNTs/T-paper. Because of the interesting advantages of this novel hybrid material such as the compatibility with paper materials such as arts, documents and packaging, excellent mechanical property, high transparency/invisibility as well as sensitivity to pressure changes. The designed device can be potentially exploited as a pressure sensor for anti-theft systems in

museums for protecting valuable paper-based arts (see Figure12k) and for anti-fake systems in smart packaging or precious documents(e.g. wills and birth certificates)(see Figure12l). The digital pictures of a transparent nanopaper-based art anti-theft system and its performance are shown in Figure 12m-p. As can be seen in Figure 12p, the voltage across the liquid crystal display (LCD) was obviously changed when the transparent nanopaper-based art anti-theft system was being pressed orreleased[61].

Self-standing films of native CNF have been reported by Rajala *et al*. The overall features of these films, such as microstructure, piezoelectric, physical, dielectric and electromechanical properties were systematically characterized. The fabricated CNF films, which have been sandwiched between two copper electrodes evaporated on polyethylene terephthalate (PET) substrates, were then utilized as functional materials in piezoelectric sensors with sensitivities of 4.7 to 6.4 pC/N. In this work, the sensitivity was defined as the charge generated by the piezoelectric sensor divided by the force used to excite the sensor. The characteristics of the reported CNF sensor were compared with a polyvinylidene fluoride sensor which was used as reference piezoelectric sensor. Owing to the obtained results, as a promising piezoelectric material for disposable sensors, actuators and energy generators, the authors suggested that the studied CNF can be exploited in electronics, sensing and related applications.[140]

It should be remarked that although the multifunctional character and unique properties of NCs have been successfully employed to generate novel hybrid materials and devices with extraordinary electrical behavior, the optical transparency of NCs has

scarcely been utilized to build innovative devices taking advantage of photocurrent phenomena or showing electrochromic or electroluminescent features.

CONCLUDING REMARKS AND FUTURE PERSPECTIVES

Paper-based (bio)sensors such as dipstick, lateral flow assay and micro-fluidic paper based analytical devices, have received great attention as they allow for low-cost, portable and disposable platforms. The main advantages of conventional paper include versatility, high abundance, flexibility and low cost offered by a porous matrix.[2,133,141–145]On the other hand, conventional paper also carries some drawbacks such as large surface roughness, optical opaqueness, low mechanicalstrength and low stability in water, which may hinder its broad integration into (opto)electronic devices and sensors. However, nanopaper, as a sheet that is completely made of NCs, not only has all the advantageous features exhibited by conventional paper, but also brings optical transparency and obviates the aforementioned drawbacks by offering much lower thermal expansion, much lower surface roughness and much higher chemical, mechanical and thermal stability[44,48,49,88–91]. Furthermore, comparing with conventional paper, nanopaper maintains its 3D structure in water. The high transparency, flexibility, functionality, thermal stability, foldability, printability and biodegradability of nanopaper facilitate a simple alternative – albeit powerful – to replace plastic and glass substrates in high-performance (opto)electronic devices such as electrodes, sensors, actuators, electrochromic devices, and so forth. These outstanding characteristics of nanopaper make this novel material an excellent substrate to create a new generation of

optical/electrical (bio)sensors. Importantly, flexibility is crucial to engineer advantageous devices in terms of size, weight, manufacturability and assembly process. In fact, extensive efforts have already been devoted to fabricate NCs-based substrates as conductive/transparent and flexible platforms that are expected to have potential applications in flexible/wearable electronics devices such as displays, sensors and actuators.[42,45,49,55,57,61,75,81,87,89,91–93,95,146,147,148149]Apart from this, several fluorescently labeled NCs have been synthesized, which are finding promising applications in the fields of (bio)sensing, bioimaging and optical labeling.[31,33,78,83,86,121,150]

NCs-based platforms are an emergent approach to fabricate advantageous, efficient, simple, cost-effective and disposable optical/electrical analytical devices for a myriad of(bio)sensing applications especially in health diagnosis, environmental monitoring, food quality control, forensic analysis and also physical sensing. Interestingly, as it can be observed in Table 1 and 2, the versatility and multifunctional character of NCs open up the opportunity to use similar composite materials such as AgNp-decorated NCs in different techniques; for instance, colorimetric, nanoplasmonics, surface enhanced Raman scattering and electrical analysis. Overall, Table 1 and 2 reflect that although similar hybrid materials based on NCs have been reported, they have multifunctional capabilities. Moreover, these tables provide an overview on the composition of the discussed composites and the opportunity to compare and contrast different approaches with the same aim (e.g. glucose biosensors or pH sensing systems), as well as their analytical performance.

Coupling of NCs as other paper-based platforms with emerging and advantageous nanomaterials, including graphene and biocompatible derivatives such as graphene-

quantum dots, may lead to interesting wearable, smart & alerting food packaging and other interesting applications compatible with mobile phone-based sensing systems.[2,151,152] Moreover, theranostic approaches could also be advantageously benefited by NCs-based hybrid materials.

All in all, with further improvements in this growing research field, we foresee that many of the (bio)sensors which are currently based on plastic, glass or paper platforms will be fabricated based on NCs platforms. In the mid/long term, NCs will be revolutionizing the state-of-the-art of the (bio)sensing technology.

Acknowledgements

H. G. and T N. acknowledge supports from ACECR-Production Technology Research Institute (Ahvaz, Iran) and Iranian Nanotechnology Initiative Council. ICN2 acknowledges support from the Severo Ochoa Program (MINECO, Grant SEV-2013-0295). The Nanobiosensors and Bioelectronics Group acknowledges the support from the Generalitat de Cataluña (Grant 2014 SGR 260). E. M-N. acknowledges the support from National System of Researchers, CONACYT (Mexico, Grant 74314).

Abbreviations:

2D	*two-dimensional*
3D	*three-dimensional*
4-FBT	*4-fluorobenzenethiol*
AgNP	*silver nanoparticle*
ATZ	*herbicide atrazine*
AuNP	*gold nanoparticle*
BC	*bacterial cellulose*
BNC	*bacterial nanocellulose*
CBZ	*Carbamazepine*
CCNC	*carboxylated cellulose nanocrystal*
CLNP	*Clonazepam*
CNC	*cellulose nanocrystal*
CNF	*cellulose nanofibers*
CNP	*carbon nanoparticle*
DAN	*Danofloxacin*
DNT	*2,4-dinitrotoluene*
DPASV	*differential pulse anodic stripping voltammetry*
DWCNT	*double-walled carbon nanotube*
E. coli	*Escherichia coli*
FE-SEM	*field emission scanning electron microscopy*
FITC	*fluorescein-5-isothiocyanate*
FP-SH	*thiolated fluorogenic peptide*

FRET	*fluorescence resonance energy transfer*
GCE	*glassy carbon electrode*
GO	*graphene oxide*
GOx	*glucose oxidase*
HNE	*human neutrophil elastase*
HRP	*horseradish peroxidase*
LCD	*liquid crystal display*
LOD	*limit of detection*
LSPR	*localized surface plasmon resonance*
MBT	*2-mercaptobenzothiazole*
MCP	*Metoclopramide*
MGITC	*malachite green isothiocyanate*
m-rGO	*modified-reduced graphene oxide*
MWCNT	*multiwalled carbon nanotubes*
NAC	*nitroaromatic explosive*
NC	*Nanocellulose*
NCC	*nanocrystalline cellulose*
NF	*Nanofibers*
NFC	*nanofibrillated cellulose*
NP	*Nanoparticle*
PA	*picric acid or 2,4,6-trinitrophenol*
PAA	*phenylacetic acid*
PAMAM	*poly(amidoamine)*

PDDAC	*Poly-(diallyldimethylammonium chloride)*
PDMS	*Polydimethylsiloxan*
PE	*Polyethylene*
PET	*Polyethyleneterephthalate*
PEI	*poly(ethyleneimine)*
PEP	*Phosphoenolpyruvate*
PFO	*poly(9,9-dioctylfluorene)*
PPy	*Polypyrrole*
PVA	*polyvinyl alcohol*
QCM	*quartz crystal microbalance*
QD	*quantum dot*
R 6G	*Rhodamine 6G*
RH	*relative humidity*
SDS	*sodium dodecylsulfate*
SERS	*surface enhanced Raman scattering*
SPME	*solid phase microextraction*
T-paper	*transparent nanopaper*
TEMPO	*2,2,6,6-Tetramethylpiperidine-1-oxyl*
TNT	*2,4,6-trinitrotoluene*
UCNP	*up-conversion nanoparticle*

References

(1) Turner, A. P. F. Biosensors: Sense and Sensibility. *Chem. Soc. Rev.* **2013**, *42* (8), 3184–3196.

(2) Quesada-González, D.; Merkoçi, A. Nanoparticle-Based Lateral Flow Biosensors. *Biosens. Bioelectron.* **2015**, *73*, 47–63.

(3) de la Escosura-Muñiz, A.; Merkoçi, A. Nanochannels Preparation and Application in Biosensing. *ACS Nano* **2012**, *6* (9), 7556–7583.

(4) Baptista, F. R.; Belhout, S. A.; Giordani, S.; Quinn, S. J. Recent Developments in Carbon Nanomaterial Sensors. *Chem. Soc. Rev.* **2015**, *44* (13), 4433–4453.

(5) Holzinger, M.; Le Goff, A.; Cosnier, S. Nanomaterials for Biosensing Applications: A Review. *Front. Chem.* **2014**, *2*, 63(1-10).

(6) Li, J.; Wu, N. *Biosensors Based on Nanomaterials and Nanodevices*; CRC Press, 2013.

(7) Zhang, X.; Guo, Q.; Cui, D. Recent Advances in Nanotechnology Applied to Biosensors. *Sensors* **2009**, *9* (2), 1033–1053.

(8) Batley, G. E.; Kirby, J. K.; McLaughlin, M. J. Fate and Risks of Nanomaterials in Aquatic and Terrestrial Environments. *Acc. Chem. Res.* **2012**, *46* (3), 854–862.

(9) Hutchison, J. E. Greener Nanoscience: A Proactive Approach to Advancing Applications and Reducing Implications of Nanotechnology. *ACS Nano* **2008**, *2* (3), 395–402.

(10) Sharifi, S.; Behzadi, S.; Laurent, S.; Forrest, M. L.; Stroeve, P.; Mahmoudi, M. Toxicity of Nanomaterials. *Chem. Soc. Rev.* **2012**, *41* (6), 2323–2343.

(11) Grossman, R. F.; Nwabunma, D.; Dufresne, A.; Thomas, S.; Pothan, L. A.

Biopolymer Nanocomposites: Processing, Properties, and Applications; John Wiley & Sons, 2013; Vol. 8.

(12) Habibi, Y.; Lucia, L. A.; Rojas, O. J. Cellulose Nanocrystals: Chemistry, Self-Assembly, and Applications. *Chem. Rev.* **2010**, *110* (6), 3479–3500.

(13) Khalil, H. P. S. A.; Bhat, A. H.; Yusra, A. F. I. Green Composites from Sustainable Cellulose Nanofibrils: A Review. *Carbohydr. Polym.* **2012**, *87* (2), 963–979.

(14) Lin, N.; Huang, J.; Dufresne, A. Preparation, Properties and Applications of Polysaccharide Nanocrystals in Advanced Functional Nanomaterials: A Review. *Nanoscale* **2012**, *4* (11), 3274–3294.

(15) Lu, Y.; Ozcan, S. Green Nanomaterials: On Track for a Sustainable Future. *Nano Today* **2015**, *10* (4), 417–420.

(16) Lavoine, N.; Desloges, I.; Dufresne, A.; Bras, J. Microfibrillated cellulose–Its Barrier Properties and Applications in Cellulosic Materials: A Review. *Carbohydr. Polym.* **2012**, *90* (2), 735–764.

(17) Klemm, D.; Kramer, F.; Moritz, S.; Lindström, T.; Ankerfors, M.; Gray, D.; Dorris, A. Nanocelluloses: A New Family of Nature-Based Materials. *Angew. Chemie - Int. Ed.* **2011**, *50* (24), 5438–5466.

(18) Moon, R. J.; Martini, A.; Nairn, J.; Simonsen, J.; Youngblood, J. Cellulose Nanomaterials Review: Structure, Properties and Nanocomposites. *Chem. Soc. Rev.* **2011**, *40* (7), 3941–3994.

(19) Pandey, J. K.; Takagi, H.; Nakagaito, A. N.; Kim, H.-J. Handbook of Polymer Nanocomposites. Processing, Performance and Application Volume C: Polymer Nanocomposites of Cellulose Nanoparticles. **2015**.

(20) Thakur, V. K. *Nanocellulose Polymer Nanocomposites: Fundamentals and Applications*; John Wiley & Sons, 2014.

(21) Kalia, S.; Kaith, B. S.; Kaur, I. *Cellulose Fibers: Bio-and Nano-Polymer Composites: Green Chemistry and Technology*; Springer Science & Business Media, 2011.

(22) Khalil, H. P. S. A.; Davoudpour, Y.; Islam, M. N.; Mustapha, A.; Sudesh, K.; Dungani, R.; Jawaid, M. Production and Modification of Nanofibrillated Cellulose Using Various Mechanical Processes: A Review. *Carbohydr. Polym.* **2014**, *99*, 649–665.

(23) Eichhorn, S. J. Cellulose Nanowhiskers: Promising Materials for Advanced Applications. *Soft Matter* **2011**, *7* (2), 303–315.

(24) Wei, H.; Rodriguez, K.; Renneckar, S.; Vikesland, P. J. Environmental Science and Engineering Applications of Nanocellulose-Based Nanocomposites. *Environ. Sci. Nano* **2014**, *1* (4), 302–316.

(25) Lin, N.; Dufresne, A. Nanocellulose in Biomedicine: Current Status and Future Prospect. *Eur. Polym. J.* **2014**, *59*, 302–325.

(26) Isogai, A.; Saito, T.; Fukuzumi, H. TEMPO-Oxidized Cellulose Nanofibers. *Nanoscale* **2011**, *3* (1), 71–85.

(27) Yousefi, H.; Faezipour, M.; Hedjazi, S.; Mousavi, M. M.; Azusa, Y.; Heidari, A. H. Comparative Study of Paper and Nanopaper Properties Prepared from Bacterial Cellulose Nanofibers and Fibers/ground Cellulose Nanofibers of Canola Straw. *Ind. Crops Prod.* **2013**, *43*, 732–737.

(28) Foresti, M. L.; Vázquez, A.; Boury, B. Applications of Bacterial Cellulose as

Precursor of Carbon and Composites with Metal Oxide, Metal Sulfide and Metal Nanoparticles: A Review of Recent Advances. *Carbohydr. Polym.* **2017**, *157*, 447–467.

(29) Habibi, Y. Key Advances in the Chemical Modification of Nanocelluloses. *Chem. Soc. Rev.* **2014**, *43* (5), 1519–1542.

(30) Liew, S. Y.; Shariki, S.; Vuorema, A.; Walsh, D. A.; Marken, F.; Thielemans, W. Cellulose Nanowhiskers in Electrochemical Applications. *ACS Symp. Ser.* **2012**, *1107*, 75–106.

(31) Leung, A. C. W.; Hrapovic, S.; Lam, E.; Liu, Y.; Male, K. B.; Mahmoud, K. A.; Luong, J. H. T. Characteristics and Properties of Carboxylated Cellulose Nanocrystals Prepared from a Novel One-Step Procedure. *Small* **2011**, *7* (3), 302–305.

(32) Lam, E.; Male, K. B.; Chong, J. H.; Leung, A. C. W.; Luong, J. H. T. Applications of Functionalized and Nanoparticle-Modified Nanocrystalline Cellulose. *Trends Biotechnol.* **2012**, *30* (5), 283–290.

(33) Sunasee, R.; Hemraz, U. D.; Ckless, K. Cellulose Nanocrystals: A Versatile Nanoplatform for Emerging Biomedical Applications. *Expert Opin. Drug Deliv.* **2016**, *13 (9)*, 1243–1256.

(34) Siqueira, G.; Bras, J.; Dufresne, A. Cellulosic Bionanocomposites: A Review of Preparation, Properties and Applications. *Polymers (Basel).* **2010**, *2* (4), 728–765.

(35) Peng, B. L.; Dhar, N.; Liu, H. L.; Tam, K. C. Chemistry and Applications of Nanocrystalline Cellulose and Its Derivatives: A Nanotechnology Perspective. *Can. J. Chem. Eng.* **2011**, *89* (5), 1191–1206.

(36) Duran, N.; Paula Lemes, A.; B. Seabra, A. Review of Cellulose Nanocrystals Patents: Preparation, Composites and General Applications. *Recent Pat. Nanotechnol.* **2012**, *6* (1), 16–28.

(37) Ohkawa, K. Nanofibers of Cellulose and Its Derivatives Fabricated Using Direct Electrospinning. *Molecules* **2015**, *20* (5), 9139–9154.

(38) Kim, C.-W.; Kim, D.-S.; Kang, S.-Y.; Marquez, M.; Joo, Y. L. Structural Studies of Electrospun Cellulose Nanofibers. *Polymer (Guildf).* **2006**, *47* (14), 5097–5107.

(39) Missoum, K.; Belgacem, M. N.; Bras, J. Nanofibrillated Cellulose Surface Modification: A Review. *Materials (Basel).* **2013**, *6* (5), 1745–1766.

(40) Siró, I.; Plackett, D. Microfibrillated Cellulose and New Nanocomposite Materials: A Review. *Cellulose* **2010**, *17* (3), 459–494.

(41) Gama, M.; Gatenholm, P.; Klemm, D.; Al, E. *Bacterial NanoCellulose*; 2013.

(42) Hu, W.; Chen, S.; Yang, J.; Li, Z.; Wang, H. Functionalized Bacterial Cellulose Derivatives and Nanocomposites. *Carbohydr. Polym.* **2014**, *101*, 1043–1060.

(43) Jozala, A. F.; de Lencastre-Novaes, L. C.; Lopes, A. M.; de Carvalho Santos-Ebinuma, V.; Mazzola, P. G.; Pessoa-Jr, A.; Grotto, D.; Gerenutti, M.; Chaud, M. V. Bacterial Nanocellulose Production and Application: A 10-Year Overview. *Appl. Microbiol. Biotechnol.* **2016**, *100* (5), 2063–2072.

(44) Zhu, H.; Parvinian, S.; Preston, C.; Vaaland, O.; Ruan, Z.; Hu, L. Transparent Nanopaper with Tailored Optical Properties. *Nanoscale* **2013**, *5* (9), 3787–3792.

(45) Zhu, H.; Fang, Z.; Wang, Z.; Dai, J.; Yao, Y.; Shen, F.; Preston, C.; Wu, W.; Peng, P.; Jang, N. Extreme Light Management in Mesoporous Wood Cellulose Paper for Optoelectronics. *ACS Nano* **2015**, *10* (1), 1369–1377.

(46) Zhu, H.; Fang, Z.; Preston, C.; Li, Y.; Hu, L. Transparent Paper: Fabrications, Properties, and Device Applications. *Energy Environ. Sci.* **2014**, *7* (1), 269–287.

(47) Sehaqui, H.; Zhou, Q.; Ikkala, O.; Berglund, L. A. Strong and Tough Cellulose Nanopaper with High Specific Surface Area and Porosity. *Biomacromolecules* **2011**, *12* (10), 3638–3644.

(48) Nogi, M.; Iwamoto, S.; Nakagaito, A. N.; Yano, H. Optically Transparent Nanofiber Paper. *Adv. Mater.* **2009**, *21* (16), 1595–1598.

(49) Fang, Z.; Zhu, H.; Preston, C.; Han, X.; Li, Y.; Lee, S.; Chai, X.; Chen, G.; Hu, L. Highly Transparent and Writable Wood All-Cellulose Hybrid Nanostructured Paper. *J. Mater. Chem. C* **2013**, *1* (39), 6191–6197.

(50) Gindl-Altmutter, W.; Veigel, S.; Obersriebnig, M.; Tippelreither, C.; Keckes, J. High-Modulus Oriented Cellulose Nanopaper. *ACS Symp. Ser.* **2012**, *1107*, 3–16.

(51) Uetani, K.; Okada, T.; Oyama, H. T. Crystallite Size Effect on Thermal Conductive Properties of Nonwoven Nanocellulose Sheets. *Biomacromolecules* **2015**, *16* (7), 2220–2227.

(52) Usov, I.; Nyström, G.; Adamcik, J.; Handschin, S.; Schütz, C.; Fall, A.; Bergström, L.; Mezzenga, R. Understanding Nanocellulose Chirality and Structure-Properties Relationship at the Single Fibril Level. *Nat. Commun.* **2015**, *6*, 7564(1-11).

(53) Mariano, M.; El Kissi, N.; Dufresne, A. Cellulose Nanocrystals and Related Nanocomposites: Review of Some Properties and Challenges. *J. Polym. Sci. Part B Polym. Phys.* **2014**, *52* (12), 791–806.

(54) Eichhorn, S. J.; Dufresne, A.; Aranguren, M.; Marcovich, N. E.; Capadona, J. R.; Rowan, S. J.; Weder, C.; Thielemans, W.; Roman, M.; Renneckar, S.; Gindl, W.;

Veigel, S.; Keckes, J.; Yano, H.; Abe, K.; Nogi, M.; Nakagaito, A. N.; Mangalam, A.; Simonsen, J.; Benight, A. S.; Bismarck, A.; Berglund, L. A.; Peijs, T. *Review: Current International Research into Cellulose Nanofibres and Nanocomposites*; 2010; Vol. 45.

(55) Fang, Z.; Zhu, H.; Yuan, Y.; Ha, D.; Zhu, S.; Preston, C.; Chen, Q.; Li, Y.; Han, X.; Lee, S. Novel Nanostructured Paper with Ultrahigh Transparency and Ultrahigh Haze for Solar Cells. *Nano Lett.* **2014**, *14* (2), 765–773.

(56) Svagan, A. J.; Busko, D.; Avlasevich, Y.; Glasser, G.; Baluschev, S.; Landfester, K. Photon Energy Upconverting Nanopaper: A Bioinspired Oxygen Protection Strategy. *ACS Nano* **2014**, *8* (8), 8198–8207.

(57) Nogi, M.; Karakawa, M.; Komoda, N.; Yagyu, H.; Nge, T. T. Transparent Conductive Nanofiber Paper for Foldable Solar Cells. *Sci. Rep.* **2015**, *5*, 17254(1-7).

(58) Mautner, A.; Lee, K.-Y.; Lahtinen, P.; Hakalahti, M.; Tammelin, T.; Li, K.; Bismarck, A. Nanopapers for Organic Solvent Nanofiltration. *Chem. Commun.* **2014**, *50* (43), 5778–5781.

(59) Orsolini, P.; Michen, B.; Huch, A.; Tingaut, P.; Caseri, W. R.; Zimmermann, T. Characterization of Pores in Dense Nanopapers and Nanofibrillated Cellulose Membranes: A Critical Assessment of Established Methods. *ACS Appl. Mater. Interfaces* **2015**, *7* (46), 25884–25897.

(60) Willgert, M.; Leijonmarck, S.; Lindbergh, G.; Malmström, E.; Johansson, M. Cellulose Nanofibril Reinforced Composite Electrolytes for Lithium Ion Battery Applications. *J. Mater. Chem. A* **2014**, *2* (33), 13556–13564.

(61) Zhong, J.; Zhu, H.; Zhong, Q.; Dai, J.; Li, W.; Jang, S.-H.; Yao, Y.; Henderson, D.; Hu, Q.; Hu, L. Self-Powered Human-Interactive Transparent Nanopaper Systems. *ACS Nano* **2015**, *9* (7), 7399–7406.

(62) Wicklein, B.; Kocjan, A.; Salazar-Alvarez, G.; Carosio, F.; Camino, G.; Antonietti, M.; Bergström, L. Thermally Insulating and Fire-Retardant Lightweight Anisotropic Foams Based on Nanocellulose and Graphene Oxide. *Nat. Nanotechnol.* **2015**, *10* (3), 277–283.

(63) Salas, C.; Nypelö, T.; Rodriguez-Abreu, C.; Carrillo, C.; Rojas, O. J. Nanocellulose Properties and Applications in Colloids and Interfaces. *Curr. Opin. Colloid Interface Sci.* **2014**, *19* (5), 383–396.

(64) Díez, I.; Eronen, P.; Österberg, M.; Linder, M. B.; Ikkala, O.; Ras, R. H. A. Functionalization of Nanofibrillated Cellulose with Silver Nanoclusters: Fluorescence and Antibacterial Activity. *Macromol. Biosci.* **2011**, *11* (9), 1185–1191.

(65) Liimatainen, H.; Ezekiel, N.; Sliz, R.; Ohenoja, K.; Sirviö, J. A.; Berglund, L.; Hormi, O.; Niinimäki, J. High-Strength Nanocellulose–talc Hybrid Barrier Films. *ACS Appl. Mater. Interfaces* **2013**, *5* (24), 13412–13418.

(66) Pinto, R. J. B.; Neves, M. C.; Neto, C. P.; Trindade, T. Composites of Cellulose and Metal Nanoparticles. *Nanocomposites - New Trends Dev.* **2012**, 73–96.

(67) Hinestroza, J.; Netravali, A. N. *Cellulose Based Composites: New Green Nanomaterials*; John Wiley & Sons, 2014.

(68) Aspler, J. O. E.; Bouchard, J.; Hamad, W.; Berry, R.; Beck, S.; Drolet, F.; Zou, X. Review of Nanocellulosic Products and Their Applications. *Biopolym.*

Nanocomposites **2013**, 461–508.

(69) Oksman, K.; Aitomäki, Y.; Mathew, A. P.; Siqueira, G.; Zhou, Q.; Butylina, S.; Tanpichai, S.; Zhou, X.; Hooshmand, S. Review of the Recent Developments in Cellulose Nanocomposite Processing. *Compos. Part A Appl. Sci. Manuf.* **2016**, *83*, 2–18.

(70) Eyley, S.; Thielemans, W. Surface Modification of Cellulose Nanocrystals. *Nanoscale* **2014**, *6* (14), 7764–7779.

(71) Huang, P.; Zhao, Y.; Kuga, S.; Wu, M.; Huang, Y. A Versatile Method for Producing Functionalized Cellulose Nanofibers and Their Application. *Nanoscale* **2016**, *8* (6), 3753–3759.

(72) Dufresne, A. Nanocellulose: A New Ageless Bionanomaterial. *Mater. Today* **2013**, *16* (6), 220–227.

(73) Mounika, M.; Ravindra, K. Characterization of Nanocomposites Reinforced with Cellulose Whiskers: A Review. *Mater. Today Proc.* **2015**, *2* (4), 3610–3618.

(74) Samir MASA Dufresne A, A. F. Review of Recent Research into Cellulosic Whisker, Their Properties and Their Application in Nanocomposites Field. *Biomacromolecules* **2005**, *6*, 612–626.

(75) Shi, Z.; Phillips, G. O.; Yang, G. Nanocellulose Electroconductive Composites. *Nanoscale* **2013**, *5* (8), 3194–3201.

(76) Cai, J.; Kimura, S.; Wada, M.; Kuga, S. Nanoporous Cellulose as Metal Nanoparticles Support. *Biomacromolecules* **2009**, *10* (1), 87–94.

(77) Morales-Narváez, E.; Golmohammadi, H.; Naghdi, T.; Yousefi, H.; Kostiv, U.; Horák, D.; Pourreza, N.; Merkoçi, A. Nanopaper as an Optical Sensing Platform.

ACS Nano **2015**, *9* (7), 7296–7305.

(78) Niu, T.; Gu, Y.; Huang, J. Luminescent Cellulose Sheet Fabricated by Facile Self-Assembly of Cadmium Selenide Nanoparticles on Cellulose Nanofibres. *J. Mater. Chem.* **2011**, *21* (3), 651–656.

(79) Zhu, H.; Li, Y.; Fang, Z.; Xu, J.; Cao, F.; Wan, J.; Preston, C.; Yang, B.; Hu, L. Highly Thermally Conductive Papers with Percolative Layered Boron Nitride Nanosheets. *ACS Nano* **2014**, *8* (4), 3606–3613.

(80) Jiang, Y.; Zhao, Y.; Feng, X.; Fang, J.; Shi, L. TEMPO-Mediated Oxidized Nanocellulose Incorporating with Its Derivatives of Carbon Dots for Luminescent Hybrid Films. *RSC Adv.* **2016**, *6*, 6504–6510.

(81) Chu, G.; Wang, X.; Yin, H.; Shi, Y.; Jiang, H.; Chen, T.; Gao, J.; Qu, D.; Xu, Y.; Ding, D. Free-Standing Optically Switchable Chiral Plasmonic Photonic Crystal Based on Self-Assembled Cellulose Nanorods and Gold Nanoparticles. *ACS Appl. Mater. Interfaces* **2015**, *7* (39), 21797–21806.

(82) Zhang, Y.; Carbonell, R. G.; Rojas, O. J. Bioactive Cellulose Nanofibrils for Specific Human IgG Binding. *Biomacromolecules* **2013**, *14* (12), 4161–4168.

(83) Zhao, J.; Wei, Z.; Feng, X.; Miao, M.; Sun, L.; Cao, S.; Shi, L.; Fang, J. Luminescent and Transparent Nanopaper Based on Rare-Earth Up-Converting Nanoparticle Grafted Nanofibrillated Cellulose Derived from Garlic Skin. *ACS Appl. Mater. Interfaces* **2014**, *6* (17), 14945–14951.

(84) Uth, C.; Zielonka, S.; Hoerner, S.; Rasche, N.; Plog, A.; Orelma, H.; Avrutina, O.; Zhang, K.; Kolmar, H. A Chemoenzymatic Approach to Protein Immobilization onto Crystalline Cellulose Nanoscaffolds. *Angew. Chemie Int. Ed.* **2014**, *53* (46),

12618–12623.

(85) Pourreza, N.; Golmohammadi, H.; Naghdi, T.; Yousefi, H. Green in-Situ Synthesized Silver Nanoparticles Embedded in Bacterial Cellulose Nanopaper as a Bionanocomposite Plasmonic Sensor. *Biosens. Bioelectron.* **2015**, *74*, 353–359.

(86) Xue, J.; Song, F.; Yin, X.; Wang, X.; Wang, Y. Let It Shine: A Transparent and Photoluminescent Foldable Nanocellulose/quantum Dot Paper. *ACS Appl. Mater. Interfaces* **2015**, *7* (19), 10076–10079.

(87) Olsson, R. T.; Samir, M. A. S. A.; Salazar-Alvarez, G.; Belova, L.; Ström, V.; Berglund, L. A.; Ikkala, O.; Nogues, J.; Gedde, U. W. Making Flexible Magnetic Aerogels and Stiff Magnetic Nanopaper Using Cellulose Nanofibrils as Templates. *Nat. Nanotechnol.* **2010**, *5* (8), 584–588.

(88) Inui, T.; Koga, H.; Nogi, M.; Komoda, N.; Suganuma, K. A Miniaturized Flexible Antenna Printed on a High Dielectric Constant Nanopaper Composite. *Adv. Mater.* **2015**, *27* (6), 1112–1116.

(89) Bao, W.; Fang, Z.; Wan, J.; Dai, J.; Zhu, H.; Han, X.; Yang, X.; Preston, C.; Hu, L. Aqueous Gating of van Der Waals Materials on Bilayer Nanopaper. *ACS Nano* **2014**, *8* (10), 10606–10612.

(90) Hamedi, M. M.; Hajian, A.; Fall, A. B.; Håkansson, K.; Salajkova, M.; Lundell, F.; Wågberg, L.; Berglund, L. A. Highly Conducting, Strong Nanocomposites Based on Nanocellulose-Assisted Aqueous Dispersions of Single-Wall Carbon Nanotubes. *ACS Nano* **2014**, *8* (3), 2467–2476.

(91) Huang, J.; Zhu, H.; Chen, Y.; Preston, C.; Rohrbach, K.; Cumings, J.; Hu, L. Highly Transparent and Flexible Nanopaper Transistors. *ACS Nano* **2013**, *7* (3),

2106–2113.

(92) Koga, H.; Saito, T.; Kitaoka, T.; Nogi, M.; Suganuma, K.; Isogai, A. Transparent, Conductive, and Printable Composites Consisting of TEMPO-Oxidized Nanocellulose and Carbon Nanotube. *Biomacromolecules* **2013**, *14* (4), 1160–1165.

(93) Xu, X.; Zhou, J.; Jiang, L.; Lubineau, G.; Ng, T.; Ooi, B. S.; Liao, H.-Y.; Shen, C.; Chen, L.; Zhu, J. Y. Highly Transparent, Low-Haze, Hybrid Cellulose Nanopaper as Electrodes for Flexible Electronics. *Nanoscale* **2016**, *8*, 12294–12306.

(94) Ye, C.; Malak, S. T.; Hu, K.; Wu, W.; Tsukruk, V. V. Cellulose Nanocrystal Microcapsules as Tunable Cages for Nano-and Microparticles. *ACS Nano* **2015**, *9* (11), 10887–10895.

(95) Ye, T.-N.; Lv, L.-B.; Xu, M.; Zhang, B.; Wang, K.-X.; Su, J.; Li, X.-H.; Chen, J.-S. Hierarchical Carbon Nanopapers Coupled with Ultrathin MoS 2 Nanosheets: Highly Efficient Large-Area Electrodes for Hydrogen Evolution. *Nano Energy* **2015**, *15*, 335–342.

(96) Zhang, T.; Wang, W.; Zhang, D.; Zhang, X.; Ma, Y.; Zhou, Y.; Qi, L. Biotemplated Synthesis of Gold Nanoparticle–bacteria Cellulose Nanofiber Nanocomposites and Their Application in Biosensing. *Adv. Funct. Mater.* **2010**, *20* (7), 1152–1160.

(97) Farjana, S.; Toomadj, F.; Lundgren, P.; Sanz-Velasco, A.; Naboka, O.; Enoksson, P. Conductivity-Dependent Strain Response of Carbon Nanotube Treated Bacterial Nanocellulose. *J. Sensors* **2013**, *2013*, 741248(1-7).

(98) Marques, P. A. A. P.; Nogueira, H. I. S.; Pinto, R. J. B.; Neto, C. P.; Trindade, T. Silver-Bacterial Cellulosic Sponges as Active SERS Substrates. *J. Raman*

Spectrosc. **2008**, *39* (4), 439–443.

(99) Morales-Narváez, E.; Golmohammadi, H.; Naghdi, T.; Yousefi, H.; Kostiv, U.; Horák, D.; Pourreza, N.; Merkoçi, A. Nanopaper as an Optical Sensing Platform. *ACS Nano* **2015**, *9* (7), 7296–7305.

(100) Park, M.; Chang, H.; Jeong, D. H.; Hyun, J. Spatial Deformation of Nanocellulose Hydrogel Enhances SERS. *BioChip J.* **2013**, *7* (3), 234–241.

(101) Wei, H.; Rodriguez, K.; Renneckar, S.; Leng, W.; Vikesland, P. J. Preparation and Evaluation of Nanocellulose–gold Nanoparticle Nanocomposites for SERS Applications. *Analyst* **2015**, *140* (16), 5640–5649.

(102) Wei, H.; Vikesland, P. J. pH-Triggered Molecular Alignment for Reproducible SERS Detection via an AuNP/Nanocellulose Platform. *Sci. Rep.* **2015**, *5*, 18131(1-10).

(103) Marques, P. A. A. P.; Nogueira, H. I. S.; Pinto, R. J. B.; Neto, C. P.; Trindade, T. Silver-Bacterial Cellulosic Sponges as Active SERS Substrates. *J. Raman Spectrosc.* **2008**, *39* (4), 439–443.

(104) Nielsen, L. J.; Eyley, S.; Thielemans, W.; Aylott, J. W. Dual Fluorescent Labelling of Cellulose Nanocrystals for pH Sensing. *Chem. Commun.* **2010**, *46* (47), 8929–8931.

(105) Devarayan, K.; Kim, B.-S. Reversible and Universal pH Sensing Cellulose Nanofibers for Health Monitor. *Sensors Actuators B Chem.* **2015**, *209*, 281–286.

(106) Chen, L.; Cao, W.; Grishkewich, N.; Berry, R. M.; Tam, K. C. Synthesis and Characterization of pH-Responsive and Fluorescent Poly (Amidoamine) Dendrimer-Grafted Cellulose Nanocrystals. *J. Colloid Interface Sci.* **2015**, *450*,

101–108.

(107) Tang, L.; Li, T.; Zhuang, S.; Lu, Q.; Li, P.; Huang, B. Synthesis of pH-Sensitive Fluorescein Grafted Cellulose Nanocrystals with an Amino Acid Spacer. *ACS Sustain. Chem. Eng.* **2016**, *4* (9), 4842–4849.

(108) Wang, X.; Guo, Y.; Li, D.; Chen, H.; Sun, R. Fluorescent Amphiphilic Cellulose Nanoaggregates for Sensing Trace Explosives in Aqueous Solution. *Chem. Commun.* **2012**, *48* (45), 5569–5571.

(109) Edwards, J. V.; Prevost, N.; Sethumadhavan, K.; Ullah, A.; Condon, B. Peptide Conjugated Cellulose Nanocrystals with Sensitive Human Neutrophil Elastase Sensor Activity. *Cellulose* **2013**, *20* (3), 1223–1235.

(110) Edwards, J. V.; Prevost, N.; French, A.; Concha, M.; DeLucca, A.; Wu, Q. Nanocellulose-Based Biosensors: Design, Preparation, and Activity of Peptide-Linked Cotton Cellulose Nanocrystals Having Fluorimetric and Colorimetric Elastase Detection Sensitivity. *Engineering* **2013**, *5*, 20–28.

(111) Schyrr, B.; Pasche, S.; Voirin, G.; Weder, C.; Simon, Y. C.; Foster, E. J. Biosensors Based on Porous Cellulose Nanocrystal–poly (Vinyl Alcohol) Scaffolds. *ACS Appl. Mater. Interfaces* **2014**, *6* (15), 12674–12683.

(112) Zhou, J.; Butchosa, N.; Jayawardena, H. S. N.; Park, J.; Zhou, Q.; Yan, M.; Ramström, O. Synthesis of Multifunctional Cellulose Nanocrystals for Lectin Recognition and Bacterial Imaging. *Biomacromolecules* **2015**, *16* (4), 1426–1432.

(113) Heli, B.; Morales-Narváez, E.; Golmohammadi, H.; Ajji, A.; Merkoçi, A. Modulation of Population Density and Size of Silver Nanoparticles Embedded in Bacterial Cellulose via Ammonia Exposure: Visual Detection of Volatile Compounds in a

Piece of Plasmonic Nanopaper. *Nanoscale* **2016**, *8* (15), 7984–7991.

(114) Ruiz-Palomero, C.; Soriano, M. L.; Valcárcel, M. β-Cyclodextrin Decorated Nanocellulose: A Smart Approach towards the Selective Fluorimetric Determination of Danofloxacin in Milk Samples. *Analyst* **2015**, *140* (10), 3431–3438.

(115) Ruiz-Palomero, C.; Soriano, M. L.; Valcárcel, M. Gels Based on Nanocellulose with Photosensitive Ruthenium Bipyridine Moieties as Sensors for Silver Nanoparticles in Real Samples. *Sensors Actuators B Chem.* **2016**, *229*, 31–37.

(116) Jie Liu, Eden Morales-Narváez, Jahir Orozco, Teresa Vicent, G. and A. M. Bioluminescent Nanopaper for the Fast Screening of Toxic Substances. *Nano Res.* **2017**.

(117) Dong, S.; Roman, M. Fluorescently Labeled Cellulose Nanocrystals for Bioimaging Applications. *J. Am. Chem. Soc.* **2007**, *129* (45), 13810–13811.

(118) Dong, S.; Cho, H. J.; Lee, Y. W.; Roman, M. Synthesis and Cellular Uptake of Folic Acid-Conjugated Cellulose Nanocrystals for Cancer Targeting. *Biomacromolecules* **2014**, *15* (5), 1560–1567.

(119) Grate, J. W.; Mo, K.-F.; Shin, Y.; Vasdekis, A.; Warner, M. G.; Kelly, R. T.; Orr, G.; Hu, D.; Dehoff, K. J.; Brockman, F. J. Alexa Fluor-Labeled Fluorescent Cellulose Nanocrystals for Bioimaging Solid Cellulose in Spatially Structured Microenvironments. *Bioconjug. Chem.* **2015**, *26* (3), 593–601.

(120) Colombo, L.; Zoia, L.; Violatto, M. B.; Previdi, S.; Talamini, L.; Sitia, L.; Nicotra, F.; Orlandi, M.; Salmona, M.; Recordati, C. Organ Distribution and Bone Tropism of Cellulose Nanocrystals in Living Mice. *Biomacromolecules* **2015**, *16* (9), 2862–

2871.

(121) Navarro, J. R. G.; Wennmalm, S.; Godfrey, J.; Breitholtz, M.; Edlund, U. Luminescent Nanocellulose Platform: From Controlled Graft Block Copolymerization to Biomarker Sensing. *Biomacromolecules* **2016**, *17* (3), 1101–1109.

(122) Bonne, M. J.; Edler, K. J.; Buchanan, J. G.; Wolverson, D.; Psillakis, E.; Helton, M.; Thielemans, W.; Marken, F. Thin-Film Modified Electrodes with Reconstituted Cellulose-PDDAC Films for the Accumulation and Detection of Triclosan. *J. Phys. Chem. C* **2008**, *112* (7), 2660–2666.

(123) Tsourounaki, K.; Bonne, M. J.; Thielemans, W.; Psillakis, E.; Helton, M.; McKee, A.; Marken, F. Nanofibrillar Cellulose-Chitosan Composite Film Electrodes: Competitive Binding of Triclosan, Fe (CN) 63−/4−, and SDS Surfactant. *Electroanalysis* **2008**, *20* (22), 2395–2402.

(124) Wang, W.; Li, H.; Zhang, D.; Jiang, J.; Cui, Y.; Qiu, S.; Zhou, Y.; Zhang, X. Fabrication of Bienzymatic Glucose Biosensor Based on Novel Gold Nanoparticles-Bacteria Cellulose Nanofibers Nanocomposite. *Electroanalysis* **2010**, *22* (21), 2543–2550.

(125) Wang, W.; Zhang, T.-J.; Zhang, D.-W.; Li, H.-Y.; Ma, Y.-R.; Qi, L.-M.; Zhou, Y.-L.; Zhang, X.-X. Amperometric Hydrogen Peroxide Biosensor Based on the Immobilization of Heme Proteins on Gold Nanoparticles–bacteria Cellulose Nanofibers Nanocomposite. *Talanta* **2011**, *84* (1), 71–77.

(126) Dong, L.; Zhang, X.; Ren, S.; Lei, T.; Sun, X.; Qi, Y.; Wu, Q. Poly(diallyldimethylammonium Chloride)–cellulose Nanocrystals Supported Au

Nanoparticles for Nonenzymatic Glucose Sensing. *RSC Adv.* **2016**, *6*, 6436–6442.

(127) Esmaeili, C.; Abdi, M. M.; Mathew, A. P.; Jonoobi, M.; Oksman, K.; Rezayi, M. Synergy Effect of Nanocrystalline Cellulose for the Biosensing Detection of Glucose. *Sensors* **2015**, *15* (10), 24681–24697.

(128) Liu, H.; Wang, D.; Song, Z.; Shang, S. Preparation of Silver Nanoparticles on Cellulose Nanocrystals and the Application in Electrochemical Detection of DNA Hybridization. *Cellulose* **2011**, *18* (1), 67–74.

(129) Liu, H.; Wang, D.; Shang, S.; Song, Z. Synthesis and Characterization of Ag–Pd Alloy Nanoparticles/carboxylated Cellulose Nanocrystals Nanocomposites. *Carbohydr. Polym.* **2011**, *83* (1), 38–43.

(130) Hu, W.; Chen, S.; Liu, L.; Ding, B.; Wang, H. Formaldehyde Sensors Based on Nanofibrous Polyethyleneimine/bacterial Cellulose Membranes Coated Quartz Crystal Microbalance. *Sensors Actuators B Chem.* **2011**, *157* (2), 554–559.

(131) Hu, W.; Chen, S.; Zhou, B.; Liu, L.; Ding, B.; Wang, H. Highly Stable and Sensitive Humidity Sensors Based on Quartz Crystal Microbalance Coated with Bacterial Cellulose Membrane. *Sensors Actuators B Chem.* **2011**, *159* (1), 301–306.

(132) Amjadi, M.; Kyung, K.; Park, I.; Sitti, M. Stretchable, Skin-Mountable, and Wearable Strain Sensors and Their Potential Applications: A Review. *Adv. Funct. Mater.* **2016**.

(133) Li, X.; Ballerini, D. R.; Shen, W. A Perspective on Paper-Based Microfluidics: Current Status and Future Trends. *Biomicrofluidics* **2012**, *6* (1), 11301–11313.

(134) Tang, W.; Yan, T.; Ping, J.; Wu, J.; Ying, Y. Rapid Fabrication of Flexible and Stretchable Strain Sensor by Chitosan-Based Water Ink for Plants Growth Monitoring. *Adv. Mater. Technol.* **2017**.

(135) Wang, M.; Anoshkin, I. V; Nasibulin, A. G.; Korhonen, J. T.; Seitsonen, J.; Pere, J.; Kauppinen, E. I.; Ras, R. H. A.; Ikkala, O. Modifying Native Nanocellulose Aerogels with Carbon Nanotubes for Mechanoresponsive Conductivity and Pressure Sensing. *Adv. Mater.* **2013**, *25* (17), 2428–2432.

(136) Shahrokhian, S.; Balotf, H.; Ghalkhani, M. Nano Composite Coating Based on Cellulose Nanofibers/carbon Nanoparticles: Application to Voltammetric Determination of Clonazepam. *J. Solid State Electrochem.* **2015**, *19* (1), 251–260.

(137) Shahrokhian, S.; Naderi, L.; Ghalkhani, M. Nanocellulose/Carbon Nanoparticles Nanocomposite Film Modified Electrode for Durable and Sensitive Electrochemical Determination of Metoclopramide. *Electroanalysis* **2015**, *27* (11), 2637–2644.

(138) Sadasivuni, K. K.; Kafy, A.; Zhai, L.; Ko, H.; Mun, S.; Kim, J. Transparent and Flexible Cellulose Nanocrystal/reduced Graphene Oxide Film for Proximity Sensing. *small* **2015**, *11* (8), 994–1002.

(139) Yan, C.; Wang, J.; Kang, W.; Cui, M.; Wang, X.; Foo, C. Y.; Chee, K. J.; Lee, P. S. Highly Stretchable Piezoresistive Graphene–nanocellulose Nanopaper for Strain Sensors. *Adv. Mater.* **2014**, *26* (13), 2022–2027.

(140) Rajala, S.; Siponkoski, T.; Sarlin, E.; Mettänen, M.; Vuoriluoto, M.; Pammo, A.; Juuti, J.; Rojas, O. J.; Franssila, S.; Tuukkanen, S. Cellulose Nanofibril Film as a Piezoelectric Sensor Material. *ACS Appl. Mater. Interfaces* **2016**, *8* (24), 15607–

15614.

(141) Yetisen, A. K.; Akram, M. S.; Lowe, C. R. Paper-Based Microfluidic Point-of-Care Diagnostic Devices. *Lab Chip* **2013**, *13* (12), 2210–2251.

(142) Liana, D. D.; Raguse, B.; Gooding, J. J.; Chow, E. Recent Advances in Paper-Based Sensors. *Sensors* **2012**, *12* (9), 11505–11526.

(143) Parolo, C.; Merkoçi, A. Paper-Based Nanobiosensors for Diagnostics. *Chem. Soc. Rev.* **2013**, *42* (2), 450–457.

(144) Ballerini, D. R.; Li, X.; Shen, W. Patterned Paper and Alternative Materials as Substrates for Low-Cost Microfluidic Diagnostics. *Microfluid. Nanofluidics* **2012**, *13* (5), 769–787.

(145) Mahadeva, S. K.; Walus, K.; Stoeber, B. Paper as a Platform for Sensing Applications and Other Devices: A Review. *ACS Appl. Mater. Interfaces* **2015**, *7* (16), 8345–8362.

(146) Csoka, L.; Hoeger, I. C.; Rojas, O. J.; Peszlen, I.; Pawlak, J. J.; Peralta, P. N. Piezoelectric Effect of Cellulose Nanocrystals Thin Films. *ACS Macro Lett.* **2012**, *1* (7), 867–870.

(147) Fujisaki, Y.; Koga, H.; Nakajima, Y.; Nakata, M.; Tsuji, H.; Yamamoto, T.; Kurita, T.; Nogi, M.; Shimidzu, N. Transparent Nanopaper-Based Flexible Organic Thin-Film Transistor Array. *Adv. Funct. Mater.* **2014**, *24* (12), 1657–1663.

(148) Chen, J.; Akin, M.; Yang, L.; Jiao, L.; Cheng, F.; Lu, P.; Chen, L.; Liu, D.; Zhu, H. Transparent Electrode and Magnetic Permalloy Made from Novel Nanopaper. *ACS Appl. Mater. Interfaces* **2016**, *8* (40), 27081–27090.

(149) Kang, W.; Lin, M.; Chen, J.; Lee, P. S. Highly Transparent Conducting Nanopaper

for Solid State Foldable Electrochromic Devices. *Small* **2016**, *12*, 6370–6377.

(150) Abitbol, T.; Palermo, A.; Moran-Mirabal, J. M.; Cranston, E. D. Fluorescent Labeling and Characterization of Cellulose Nanocrystals with Varying Charge Contents. *Biomacromolecules* **2013**, *14* (9), 3278–3284.

(151) López-Marzo, A. M.; Merkoçi, A. Paper-Based Sensors and Assays: A Success of the Engineering Design and the Convergence of Knowledge Areas. *Lab Chip* **2016**, *16* (17), 3150–3176.

(152) Morales-Narváez, E.; Baptista-Pires, L.; Zamora-Gálvez, A.; Merkoçi, A. Graphene-Based Biosensors: Going Simple. *Adv. Mater.* **2017**, *29* (7), 1604905(1-7).

(153) Habibi, Y.; Goffin, A.-L.; Schiltz, N.; Duquesne, E.; Dubois, P.; Dufresne, A. Bionanocomposites Based on Poly (ε-Caprolactone)-Grafted Cellulose Nanocrystals by Ring-Opening Polymerization. *J. Mater. Chem.* **2008**, *18* (41), 5002–5010.

(154) Malainine, M. E.; Dufresne, A.; Dupeyre, D.; Mahrouz, M.; Vuong, R.; Vignon, M. R. Structure and Morphology of Cladodes and Spines of Opuntia Ficus-Indica. Cellulose Extraction and Characterisation. *Carbohydr. Polym.* **2003**, *51* (1), 77–83.

(155) Oksman, K.; Etang, J. A.; Mathew, A. P.; Jonoobi, M. Cellulose Nanowhiskers Separated from a Bio-Residue from Wood Bioethanol Production. *biomass and bioenergy* **2011**, *35* (1), 146–152.

(156) Sehaqui, H.; Zhou, Q.; Ikkala, O.; Berglund, L. A. Strong and Tough Cellulose Nanopaper with High Specific Surface Area and Porosity. *Biomacromolecules*

2011, *12* (10), 3638–3644.

(157) Jiang, F.; Hsieh, Y.-L. Amphiphilic Superabsorbent Cellulose Nanofibril Aerogels. *J. Mater. Chem. A* **2014**, *2* (18), 6337–6342.

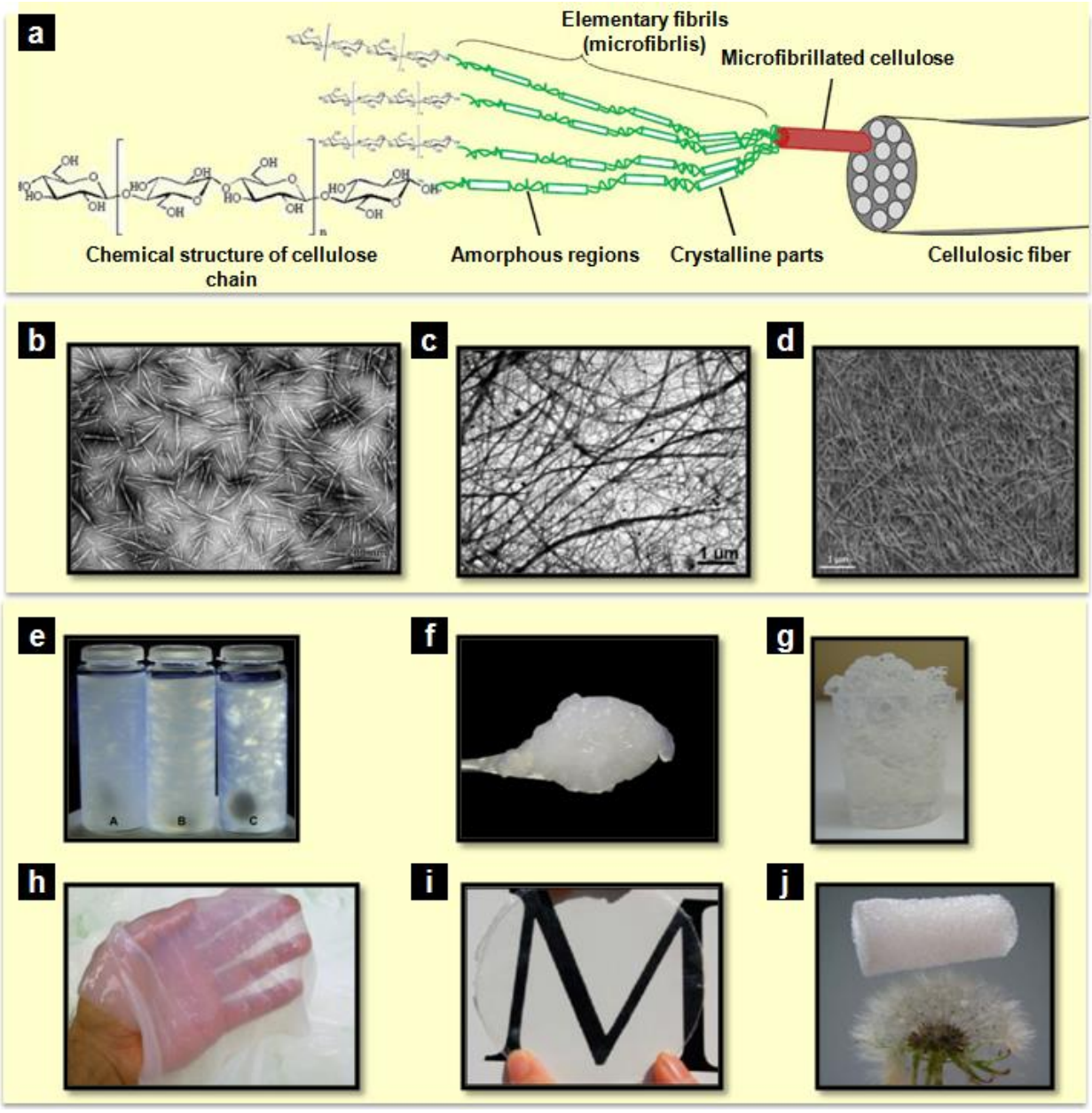

Figure 1. a) Hierarchical configuration of cellulosic fibers: from the cellulose fibers to the cellulose molecules. Reproduced with permission.[16] Copyright 2012, Elsevier. b)

Transmission electron microscopy (TEM) image of rod-like CNCs from ramie. Reprinted with permission.[153] Copyright 2008, The Royal Society of Chemistry. c) TEM image of homogenized cellulose microfibrils suspension. Reproduced with permission.[154] Copyright 2003, Elsevier. d) Scanning electron micrograph of a bare bacterial cellulose nanopaper. Reproduced with permission.[77] Copyright 2015, American Chemical Society. e) Picture of birefringence of isolated cellulose nanowhiskers suspensions (A) sonified, (B) homogenized and (C) hydrolysed.[155] Copyright 2011, Elsevier. f) Photograph of a 2 wt% microfibrillated cellulose aqueous from eucalyptus, enzymatically pre-treated. Reproduced with permission.[16] Copyright 2012, Elsevier. g) Image of a TEMPO-oxidized NFC dispersion. Reproduced with permission.[156] Copyright 2011, American Chemical Society. h) Photograph of purified nanaopaper (wet mat made completely from BCNs). Reproduced with permission.[77] Copyright 2015, American Chemical Society. i) Photograph of a transparent nanopaper made of NFC on top of “M”. Reproduced with permission.[91] Copyright 2013, American Chemical Society. j) Picture of a CNF aerogel on top of a dandelion. Reprinted with permission.[157] Copyright 2014, The Royal Society of Chemistry.

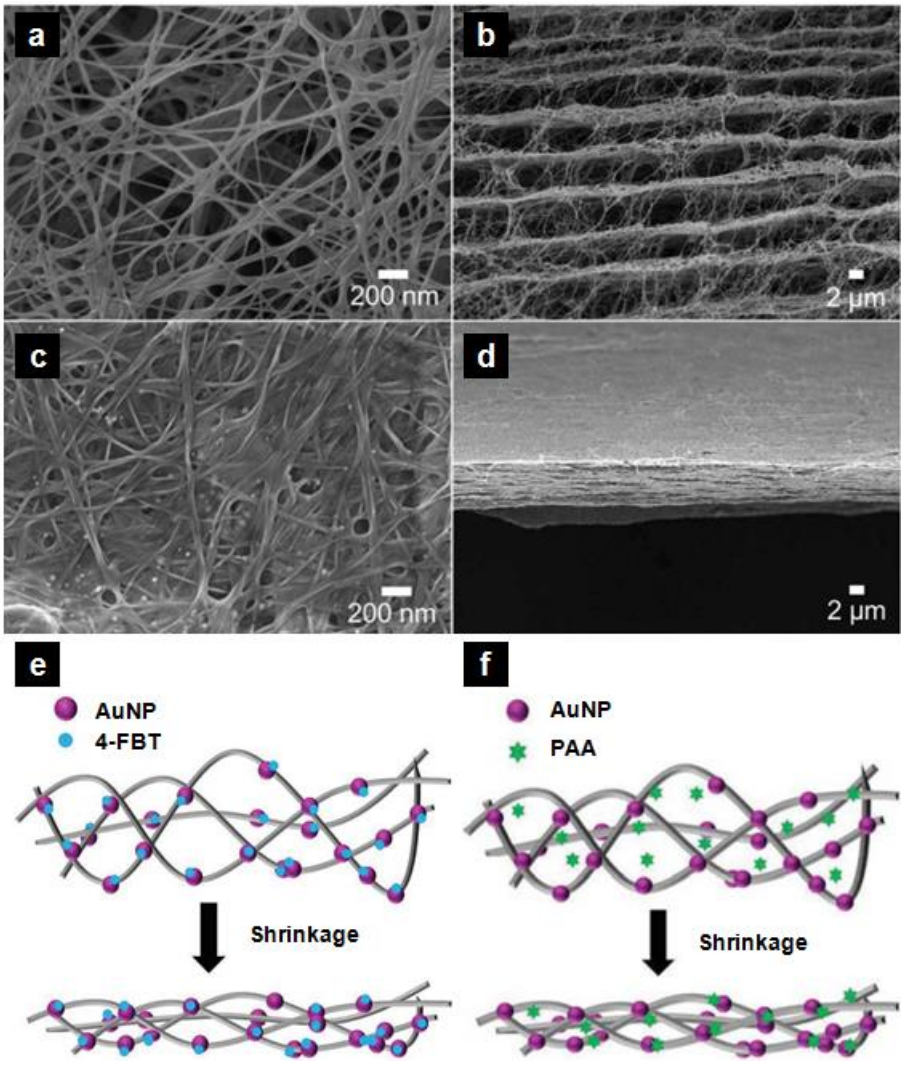

Figure2. FE-SEM images of AuNP/BC hyrogels. (a) The top view and (b) cross-sectional view of AuNP/BC hyrogels. (c) The top view and (d) cross-sectional view of spatially deformed AuNP/BC. The schematic representation for (e) 4-FBT and (f) PAA sensing by deformation of the AuNP/BC hydrogel. Reprinted with permission.[100] Copyright 2013, Springer.

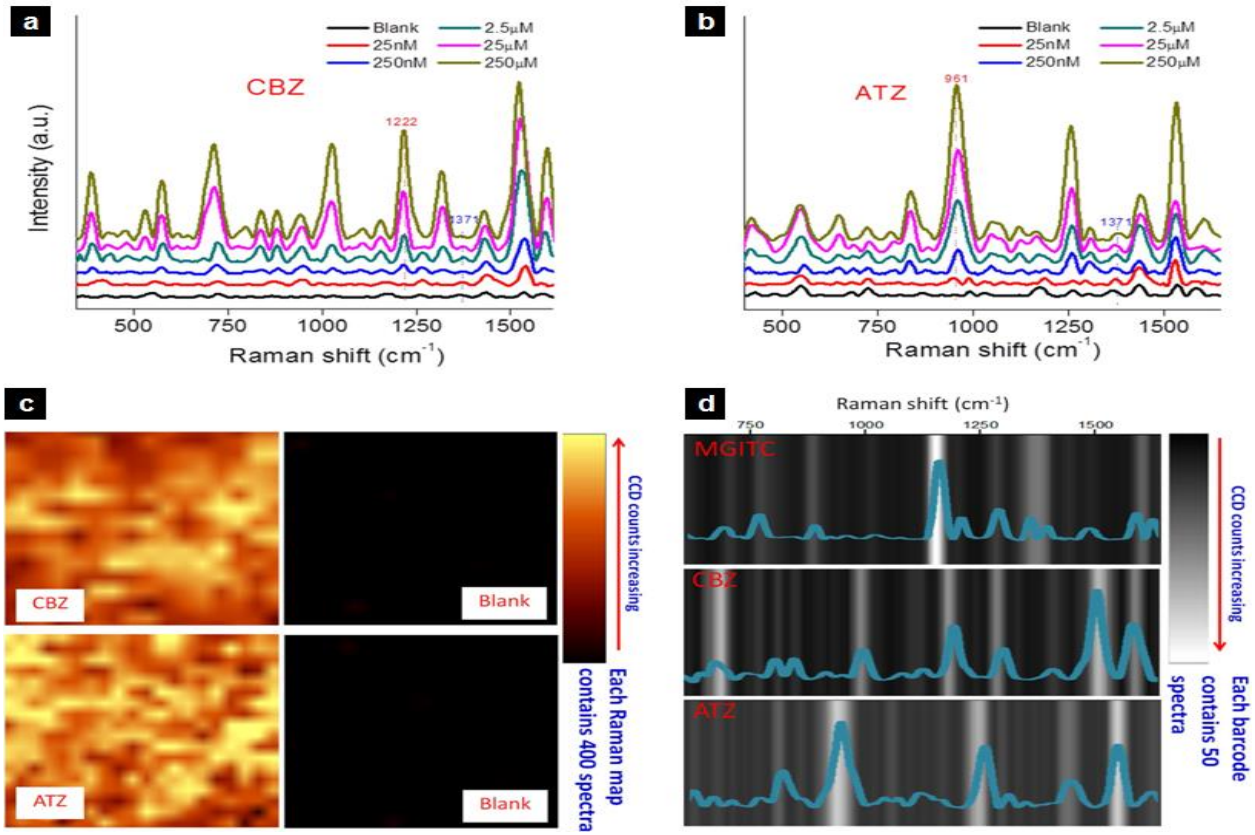

Figure 3. Average Raman spectra of AuNP/BC hydrogels for (a) CBZ and (b) ATZ in the concentration range of 25 nM–250 μM.(c) Raman XY maps of CBZ, ATZ and blank solutions on AuNP/BC; (d) SERS barcodes of 50 randomly selected spectra in a Raman map overlapping together for MGITC, CBZ and ATZ. Reproduced with permission.[102] Copyright 2015, Nature Publishing Group.

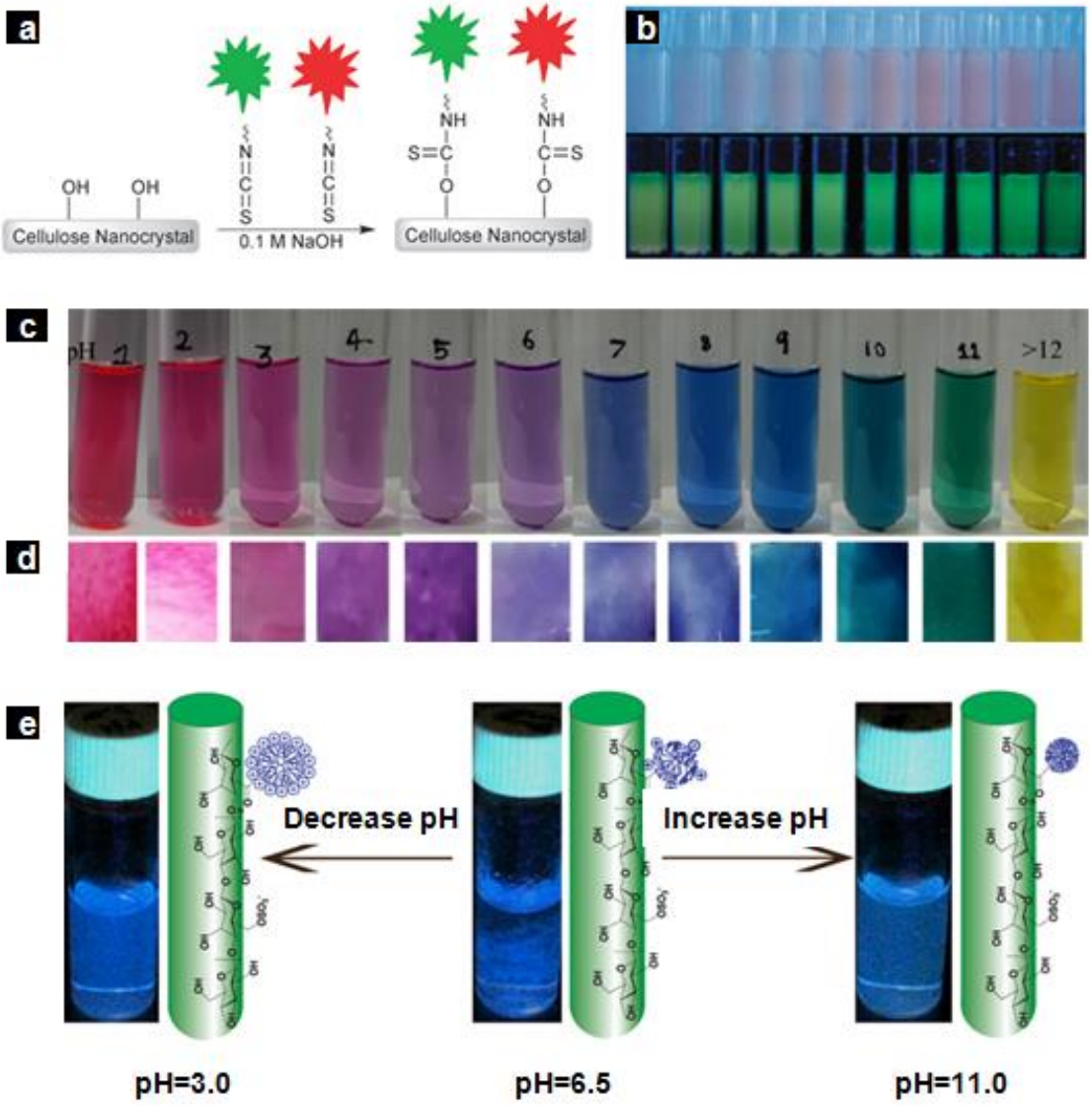

Figure 4. a) Fluorescent labelling of CNCs with isothiocyanate ester dyes and b) image of their suspensions with various pH values in the pH range of 3.5–8.0. The pH values from left to right are 3.5, 4.0, 4.5, 5.0, 5.5, 6.0, 6.5, 7.0, 7.5 and 8.0. (λex = 490 nm (top)and 540 nm (bottom)). Reprinted with permission.[104] Copyright 2010, The Royal Society of Chemistry. Photographical images of (c) the red cabbage extract solution and (d) the red cabbage CNFs at pH 1–14. Reprinted with permission.[105] Copyright 2015, Elsevier. e) Schematic description of the pH responsive and fluorescent behaviors of

PAMAM/CNC at different pH values. Reprinted with permission.[106] Copyright 2015, Elsevier.

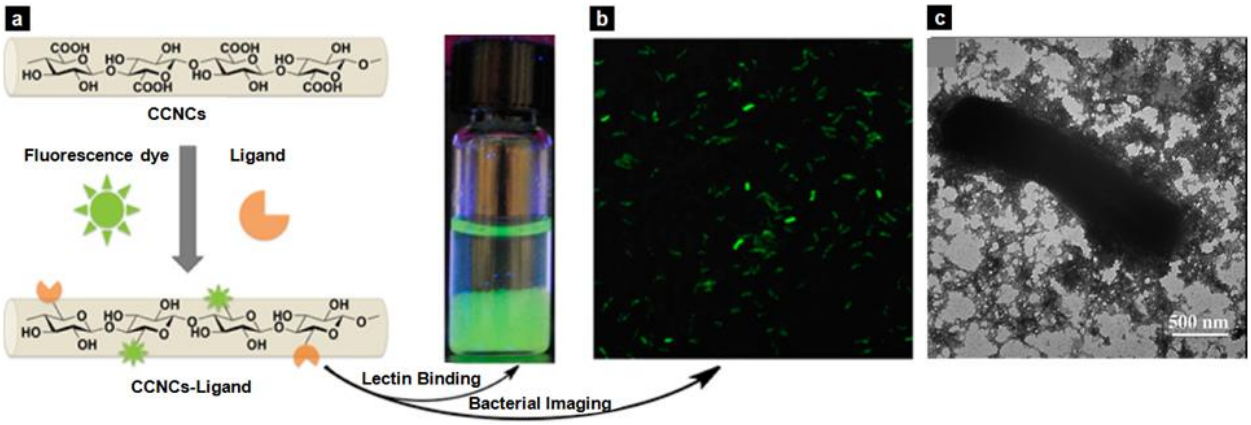

Figure 5. Schematic illustration for (a) functionalization of the CCNCs with a fluorescent dye and carbohydrate ligands and their application for lectin detection and (b) confocal fluorescence microscopy image and (c) TEM image of *E. coli* ORN 178 treated with C−CNC-mannose derivative. Reproduced with permission.[112] Copyright 2015, American Chemical Society.

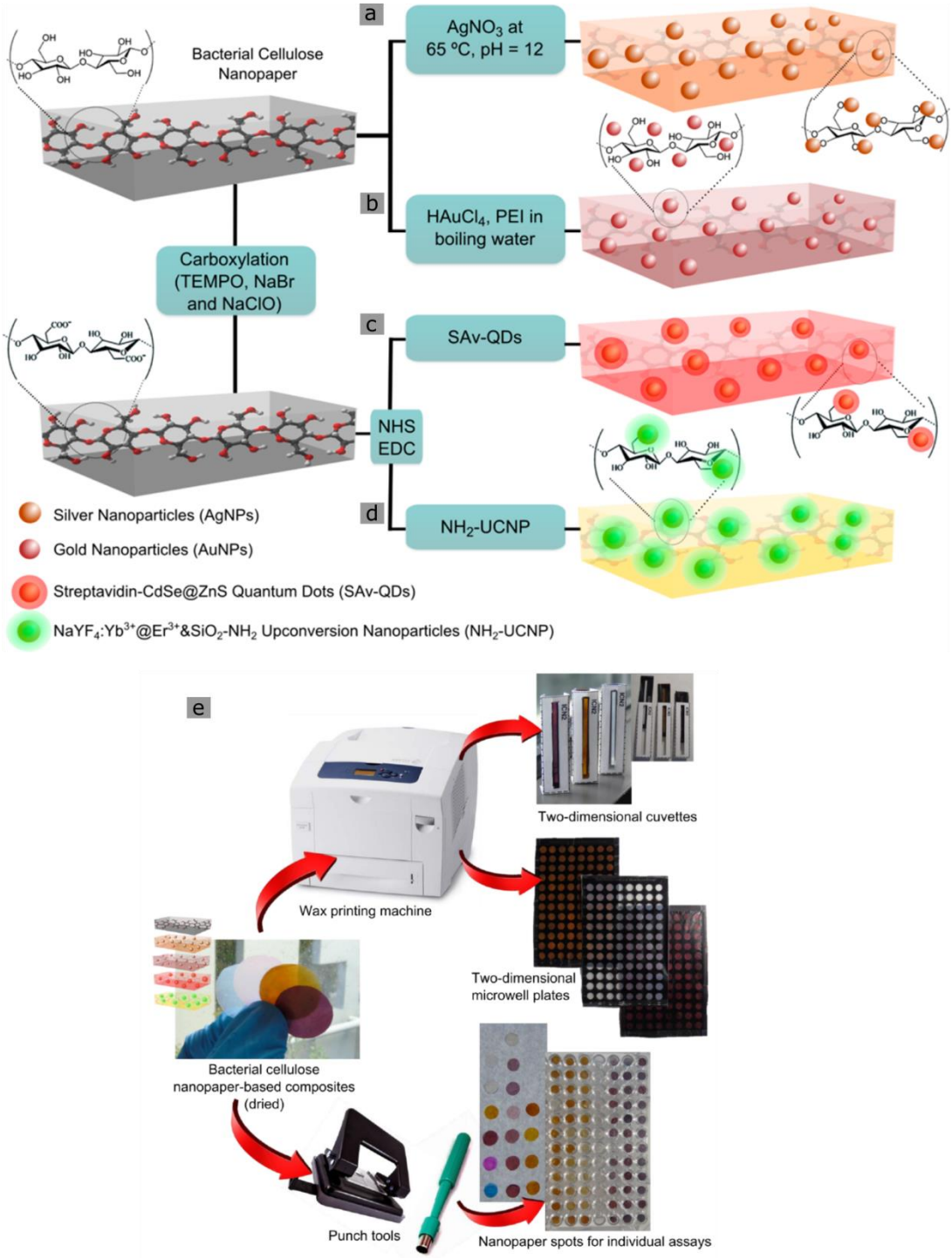

Figure 6. Schematic representation of the proposed nanopaper-based composites. (a and b) Fabrication of plasmonic nanopaper: (a) AgNP/BC; (b) AuNP/BC. (c and d) Fabrication of photoluminescent nanopaper: (c) QD/BC; (d) UCNP/BC. (e) Schematic

representation for the fabrication of nanopaper-based devices sucha s 2D cuvettes, 2D microwell plates, and spots by using a wax printing machine or punch tools. Reproduced with permission.[77] Copyright 2015, American Chemical Society.

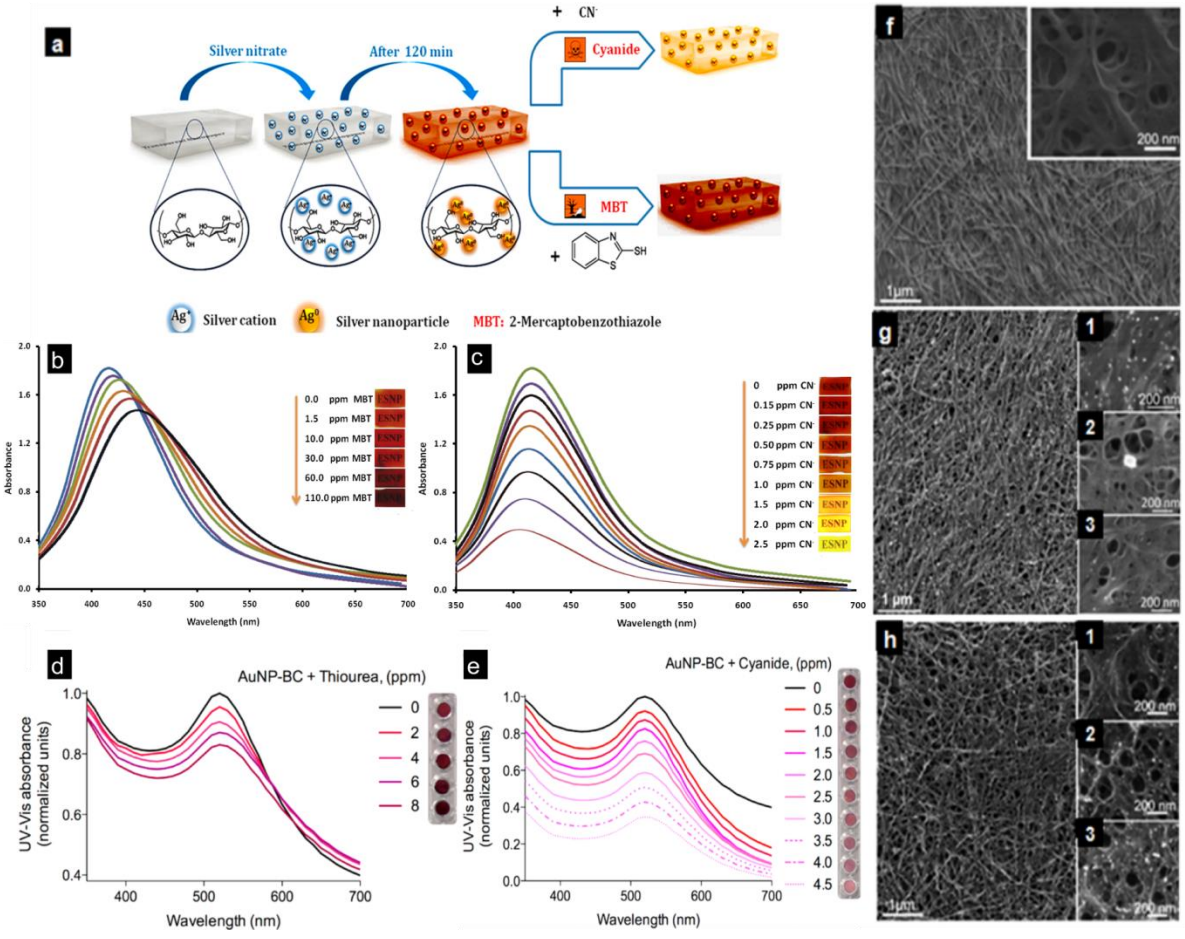

Figure 7. Schematic illustration of(a) fabrication of AgNP/BC nanopapers and their application as plasmonic chemoprobes for colorimetric sensing of cyanide and MBT. The LSPR absorption spectra of AgNP/BC nanopapers in the presence of different concentrations of (b) cyanide and (c) MBT with the corresponding changes in color.

Change in color of AuNP/BC upon addition of (d) thiourea and (e) cyanide. Scanning electron micrographs of (f) bare bacterial cellulose nanopaper, (g) AgNP/BC: (g-1) AgNPs synthesized in situ (using bacterial nanopaper as both, a reducing agent and a template); (g-2) AgNP/BCin the presence of 100 μg mL^{-1} of MBTZ; (g-3) AgNP/BC in the presence of 2 μg mL^{-1} of cyanide. Scanning electron micrographs of (h) AuNP/BC: (h-1) AuNP/BC; (h-2) AuNP/BC in the presence of 8 μg mL^{-1} of thiourea; (h-3) AuNP/BC in thepresence of 4 μgmL^{-1} of cyanide. a-c and g) Reproduced with permission.[85] Copyright 2015, Elsevier. d, e, f, h)Reproduced with permission.[77] Copyright 2015, American Chemical Society.

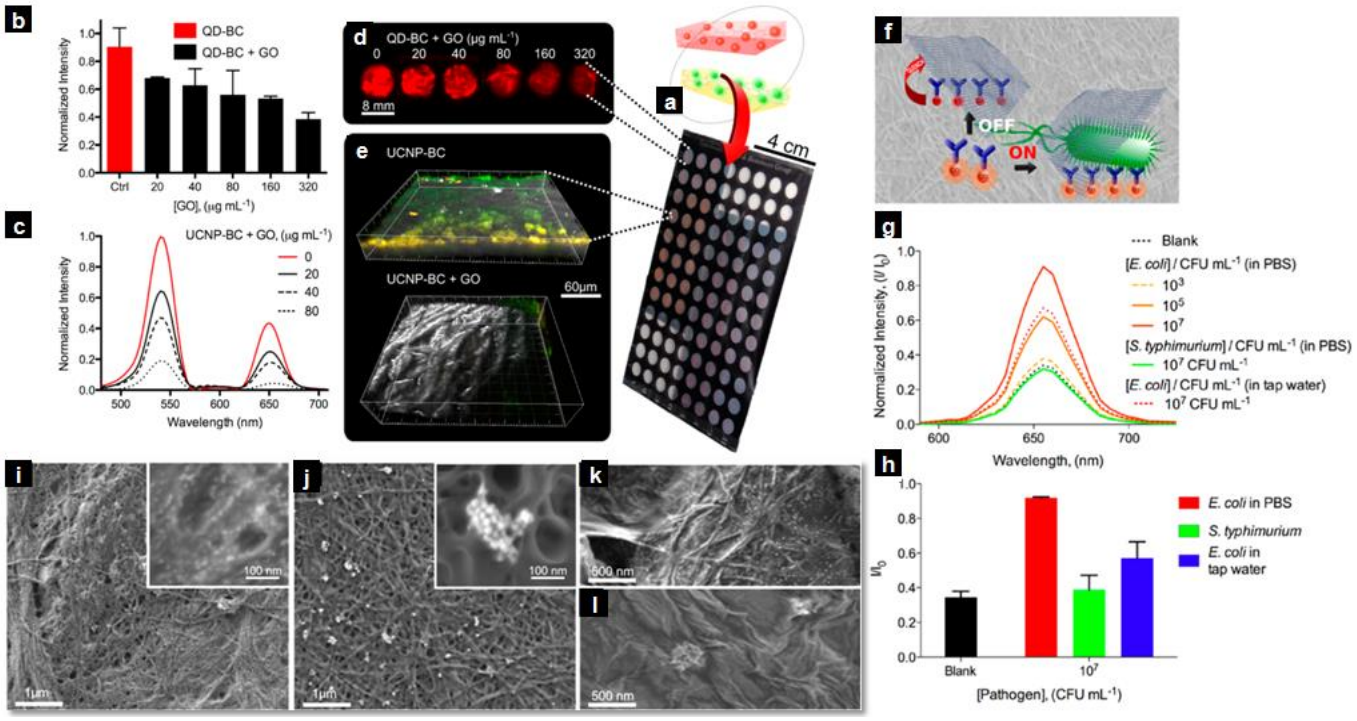

Figure 8.a) Photoluminescent nanopaper multi well plate. (b) Modulation of the photoluminescence intensity of QD/BC by addition of graphene oxide at different concentrations. (c) Image of QD/BC wells acquired using a scanner. (d) Modulation of

the photoluminescence intensity of UCNP/BC by addition of graphene oxide (GO). (e) Confocal microscopy images of UCNP/BC (top) and GO-coated UCNP/BC (bottom). Graphene oxide as a pathogen-revealing agent and antibody decorated QD/BC as a biosensing platform. (f)Schematic representation of the biosensing platform. (g) Spectra of spots for individual assays made of QD/BC (excitation wavelength 480 nm). The spectra display the photoluminescence quenching levels upon GO addition according to the analyzed sample. (h) Photoluminescence quenching levels at the maximum emission wavelength of QD/BC (655 nm) upon GO addition according to the analyzed sample. I/I_0: final photoluminescent intensity divided by starting photoluminescent intensity.(i-l)Scanning electron micrographs of the nanopaper-based platforms (performed using carbon conductive tabs as substrate). (i) Scanning electron micrographs of QDs embedded within bacterial cellulose nanopaper.(j) Scanning electron micrographs of UCNP-BC. (k) Graphene oxide-coated QD/BC. (l) Graphene oxide-coated UCNP/BC. Reproduced with permission.[77] Copyright 2015, American Chemical Society.

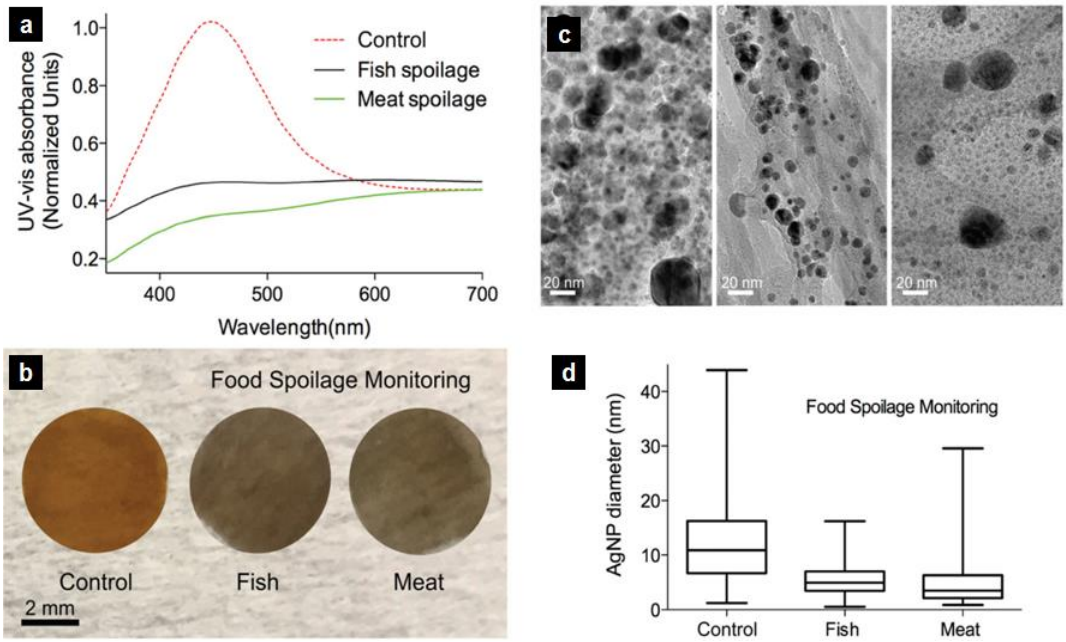

Figure 9. Food spoilage monitoring via plasmonic nanopaper. (a) UV-Vis spectra of the nanoplasmonic membranes before food spoilage exposure (Ctrl) and after food spoilage exposure (ammonia and several volatile organic compounds are released during fish and meat spoilage). (b) Appearance of the nanoplasmonic membranes before/after food spoilage monitoring. (c) TEM micrographs, from left to right: control, fish spoilage and meat spoilage. (d)Size distribution of the AgNPs embedded in the nanopaper before/after food spoilage monitoring, the box plots show the median, 25th and 75th percentiles and the extreme values of the respective size distributions (5–95 percentile).Reproduced with permission.[113] Copyright 2016, The Royal Society of Chemistry.

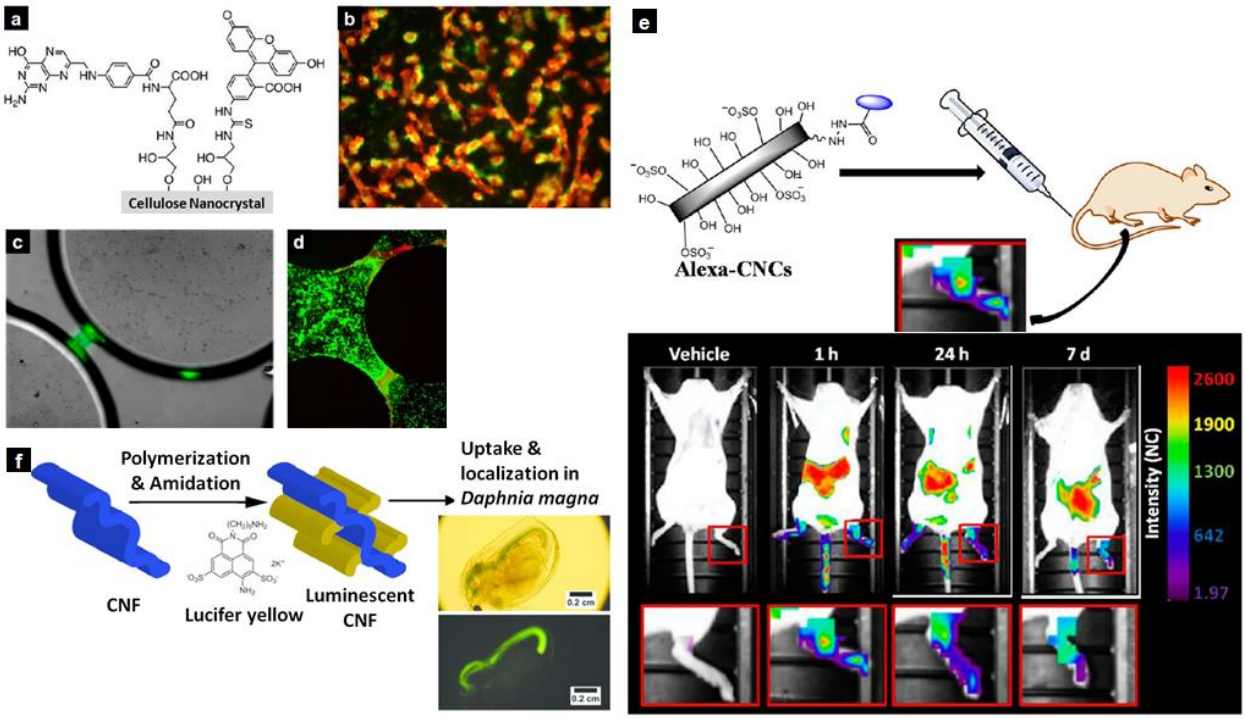

Figure 10. NCs in bioimaging. a) The structure of folic acid/FITC/CNC and b) its cellular binding/uptake by human brain tumor cells. Reprinted with permission.[118] Copyright 2014, American Chemical Society. Composite images (c) (gray: bright-field, green: Alexa Fluor 546-labeled CNCs) showing the spatial localization of the immobilized fluorescent CNCs in the pore space of a pore network micromodel. (d)Image illustrating the bacterial proliferation both on the cellulose deposits and free in a pore space (green: m Orange-expressing Flavobacterium strain, red: immobilized Alexa Fluor 647-labeled CNCs). Reprinted with permission.[119] Copyright 2015, American Chemical Society. e) Labeling of CNCs with Alexa Fluor 633 and their application for biodistribution using optical imaging of CNCs (optical fluorescence imaging before and at 1 h, 24 h, and 7 days, after intravenous CNCs injection).Reprinted with permission.[120] Copyright 2015,

American Chemical Society. f) Lucifer yellow/NC platform and its application for fluorescence-based optical sensing. CNF uptake and biodistribution in living organisms. Reprinted with permission.[121] Copyright 2016, American Chemical Society.

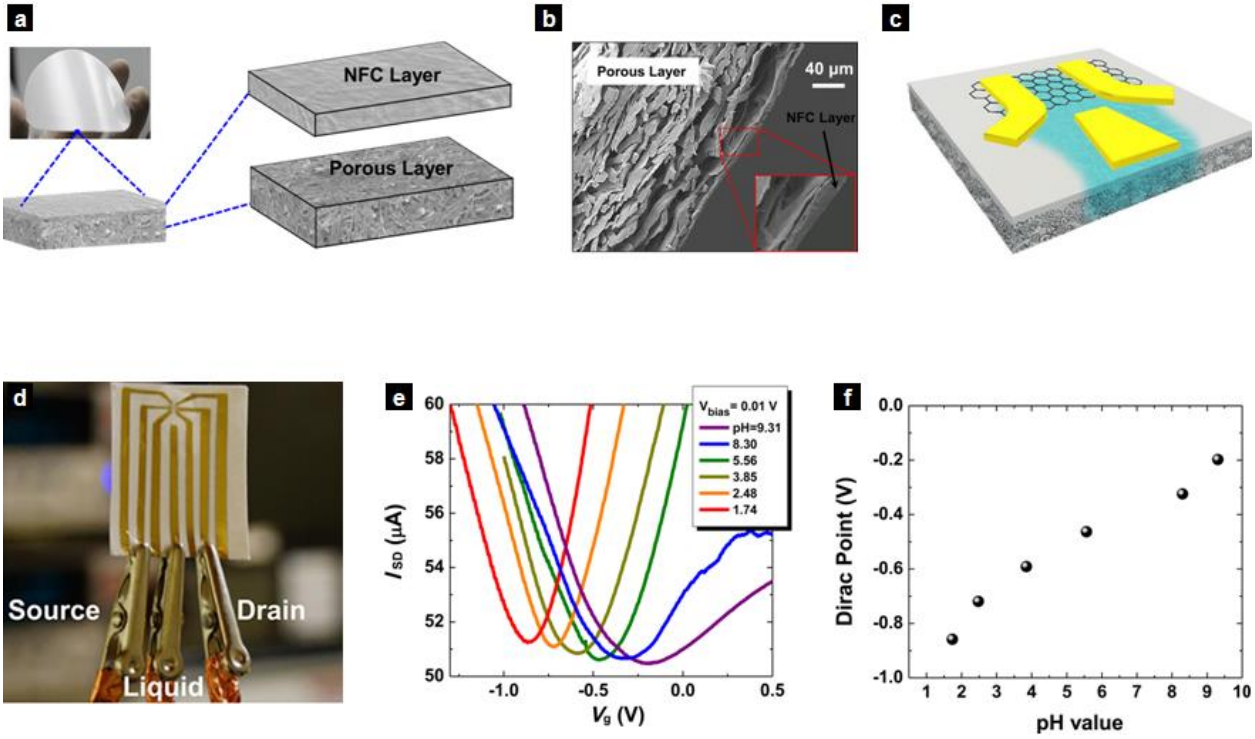

Figure 11. (a) Schematic representation of a nanopaper-based bilayer structure for the fabrication of a liquid-gated transistor and (b) Its cross-sectional FE-SEM image. (c) Schematic representation of exfoliated 2D materials deposited on a piece of bilayer mesoporous nanopaper, followed by contact electrodes fabrication (yellow).The analyzed liquid can be absorbed by the porous side (blue). (d) A typical measurement setup of the reported liquid-gated transistor. The central electrode contacts the absorbed liquid.(e) Source-drain current (*Isd*) operates as a function of gate voltage (Vg) at pH values of 1.74, 2.48, 3.85, 5.56, 8.30, and 9.31. (f) Voltage value at the Dirac

point as a function of pH value. Reproduced with permission.[89] Copyright 2014, American Chemical Society.

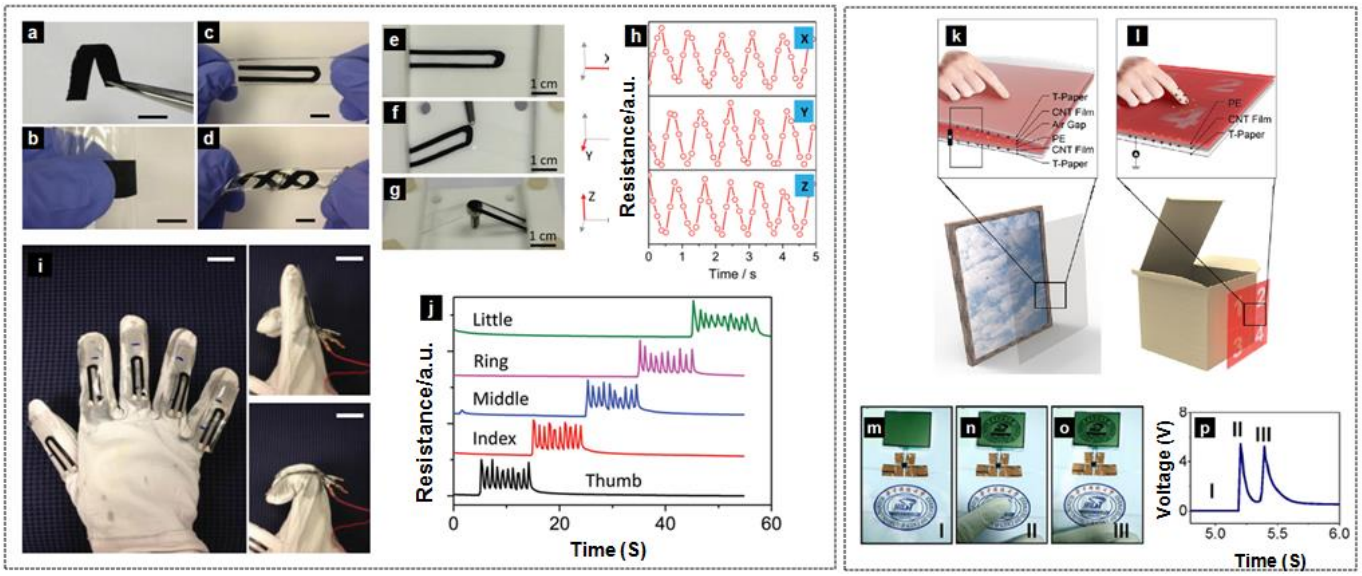

Figure 12.a–d) Example images of the free-standing flexible nanopaper (a,b) and stretchable nanopaper (c,d). The scale bars in (a–d) are 10 mm. e–g) Example Images of the graphene nanopaper sensors stretched in the X-, Y- and Z directions. h)Corresponding response curves for stretching in three directions. i and j) Wearable strain sensors for finger movement detections. i) Photographs of the data glove with five implanted sensors. The bending and stretching states of the glove finger during testing are also shown. Scale bars: 2 cm. j) Relative resistance changes for the five independent strain sensors". a-j) Reproduced with permission.[139] Copyright 2014,WILEY-VCH."Schematic diagram of (k) a transparent nanopaper-based art anti-theft system and (l) a transparent nanopaper-based smart mapping anti-fake system. (m) Digital picture of a transparent nanopaper-based art anti-theft system. Digital pictures show the LCD logo was lit up by (n) pressing motion and (o) releasing motion.

(p) The corresponding voltage across the LCD logo when it was lit up". k-p) Reproduced with permission.[61] Copyright 2015, The American Chemical Society.

Table 1. Summary of the various NC-based platforms used for optical (bio)sensing and bioimaging applications

Sensing platform	Sensing target	Sensing technique	Linearity range	LOD[a)]	[Ref.]
AgNP/BC	thiosalicylic acid, 2,2-ithiodipyridine, L-phenylalanine, L-glutamine, L-histidine	SERS	N.D.[b)] N.D. N.D. N.D. N.D.	10^{-4} M 10^{-4} M N.D. N.D. N.D.	98
AuNP/BC hydrogel	4-FBT, PAA	SERS	N.D.	N.D.	100
AuNP/BC	MGITC, R 6G	SERS	N.D.	24 molecules 78 nM	101
AuNP/BC	CBZ, ATZ, melamine, 2,4-dichloroaniline, 4-chloroaniline, 3-bromoaniline, 3-nitroaniline	SERS	0.025-250 µM 0.025-250 µM N.D. N.D. N.D. N.D. N.D.	3 nM 11 nM N.D. N.D. N.D. N.D. N.D.	102
pH-responsive dyes/CNC	pH	fluorometric	N.D.	N.D.	104
PFO/amphiphilic cellulose nanoaggregates	PA, DNT,TNT	fluorometric	N.D.	N.D.	108

peptide/CNC	HNE	fluorimetric	N.D.	0.05 U/mL	[109]
peptide/CNC	HNE	colorimetric &fluorimetric	N.D.	N.D.	[110]
fluorescein derivative/PVA/CNC	pH	fluorimetric	N.D.	N.D.	[111]
FP-SH/PVA/CNC	protease activity	fluorimetric	N.D.	N.D.	[111]
natural pigment/CNF	pH	colorimetric	1-14	N.D.	[105]
PAMAM/CNC	pH	fluorimetric	N.D.	N.D.	[106]
quinolone/CNC	Lectin	fluorimetric	N.D.	N.D.	[112]
quinolone/CNC	*E. coli*	fluorescence bioimaging	N.A.	N.A.	[112]
AgNP/BC nanopaper	MBT, Cyanide	Nanoplasmonics	2-110 μg mL^{-1} 0.2-2.5 μg mL^{-1}	1.37 μg mL^{-1} 0.012 μg mL^{-1}	[85]
AgNP/BC nanopaper	methimazole, iodide	colorimetric	0.5-10 mg L^{-1} 0.2-4 mg L^{-1}	N.D. N.D.	[77]
AuNP/BC nanopaper	thiourea, cyanide	colorimetric	2-8 mg L^{-1} 0.5-4.5 mg L^{-1}	N.D. N.D.	[77]
$NaYF4:Yb^{3+}@Er^{3+}$ UCNP/BC	GO	fluorimetric	N.D.	N.D.	[77]
CdSe@ZnSQDs/BC nanopaper	*E. coli*	fluorimetric	10^3-10^7 CFU mL^{-1}	N.D.	[77]
AgNP/BC nanopaper	Ammonia	Nanoplasmonics	N.D.	0.547 ppmv	[113]
Luminescent bacteria/BC	Diuron Tributyltin Polybrominated diphenyl ethers	Bioluminescence inhibition	N.D.	~108 μg L^{-1} ~0.24 μg L^{-1} ~8.70 μg L^{-1}	[116]
β-cyclodextrin/NC/SPME	DAN	fluorimetric	8-800 μg L^{-1}	2.5 μg L^{-1}	[114]
Ru(II) bipyridine/NC	AgNPs	fluorimetric	18.5-148 μM	11.1 μM	[115]

pH-indicator dye/ L-leucine/CNC	pH	fluorimetric	2.28-10.84	N.D.	[107]
folic acid/FITC/CNC	cancer targeting	fluorescence bioimaging	N.D.	N.D.	[118]
Alexa Fluor dye/CNC	CNCs in spatially microenvironment	fluorescence bioimaging	N.D.	N.D.	[119]
Alexa Fluor 633/CNC	interaction of CNCs with living organisms	optical bioimaging	N.D.	N.D.	[120]
lucifer yellow/CNF	CNF uptake and distribution in living organism	fluorescence bioimaging	N.D.	N.D.	[121]

[a)]LOD**:**limit of detection; [b)]N.D.**:** not described.

Table 2. Summary of the various NC-based platforms used for electrical (bio)sensing applications

Sensing platform	**Sensing target**	**Sensing technique**	**Linearity range**	**LOD[a)]**	**[Ref.]**
PDDAC/CNF/GCE	Triclosan	voltammetric	10^{-6}-10^{-3} M	N.D.[b)]	[122]
chitosan/CNF/GCE	SDS	voltammetric	N.D.	N.D.	[123]
HRP/AuNP/BC/GCE	H_2O_2	amperometric	N.D.	1 µM	[96]
HRP/AuNP/BC/GCE	H_2O_2	amperometric	0.0003–1.0 mM	0.1 µM	[125]
GOx-HRP/AuNP/BC/GCE	Glucose	amperometric	10-400 µM	2.3 µM	[124]
Au/PDDAC/CNC/GCE	Glucose	amperometric	0.004-6.5 mM	2.4 µM	[126]

GOx/PPy/CNC	Glucose	voltammetric	1.0-20 mM	0.05 mM	[127]
probe DNA/AgNP /CCNC/GCE	PAT genesequence	DPASV	1.0×10^{-10} -1.0×10^{-7} M	2.3×10^{-11}	[128]
probe DNA/Ag–Pd NPs alloy/CCNC/CPE	PEP gene sequence	DPASV	N.D.	N.D.	[129]
PEI/BC/QCM	Formaldehyde	mass sensing	1-100 μg mL^{-1}	1 μg mL^{-1}	[130]
BC/QCM	Humidity	mass sensing	20%-97% RH	N.D.	[131]
DWCNT/BC	strain	conductivity	0.034-0.39 $S.cm^{-1}$	N.D.	[97]
MWCNT/BC	strain	conductivity	0.12-1.6 $S.cm^{-1}$	N.D.	
CNT/NFC aerogel	Pressure	conductivity	N.D.	N.D.	[135]
Graphene/nanopaper	pH	electrical	N.D.	N.D.	[89]
graphene/nanopaper/PDMS	Strain	electrical	N.D.	N.D.	[139]
CNF/CNP/GCE	CLNP	voltammetric	0.1-10 μM	80 nM	[136,137]
	MCP		0.06-2 μM	6 nM	
CNC/m-rGO	proximity (human finger interface)	electrical	N.D.	N.D.	[138]
PE/CNTs/nanopaper	Pressure	electrical	N.D.	N.D.	[61]
native CNF	piezoelectric sensitivity	electrical	N.D.	N.D.	[140]

[a)]LOD**:** limit of detection; [b)]N.D.**:** not described.